



OPEN ACCESS

EDITED BY

Nicolae Corcionivoschi,
Agri-Food and Biosciences Institute,
United Kingdom

REVIEWED BY

Gratiela Gradisteanu Pircalabioru,
University of Bucharest, Romania
Igori Balta,
University of Life Sciences King Mihai I
Timișoara, Romania

*CORRESPONDENCE

Doaa Ibrahim
✉ doibrahim@vet.zu.edu.eg
Ioan Pet
✉ ioanpet@usvt.ro

RECEIVED 23 July 2024

ACCEPTED 01 November 2024

PUBLISHED 29 November 2024


CITATION

El-Hamid MIA, Ibrahim D, Abdelfattah-Hassan A, Mohammed OB, Pet I, Khalil SS, El-Badry SM, Metwally AS, Azouz AA, Elnegiry AA, Elnahriry SS, Ahmadi M and Elazab ST (2024) Silver nanoparticles loaded with pomegranate peel extract and hyaluronic acid mediate recovery of cutaneous wounds infected with *Candida albicans*. *Front. Cell. Infect. Microbiol.* 14:1469493. doi: 10.3389/fcimb.2024.1469493

COPYRIGHT

© 2024 El-Hamid, Ibrahim, Abdelfattah-Hassan, Mohammed, Pet, Khalil, El-Badry, Metwally, Azouz, Elnegiry, Elnahriry, Ahmadi and Elazab. This is an open-access article distributed under the terms of the [Creative Commons Attribution License \(CC BY\)](https://creativecommons.org/licenses/by/4.0/). The use, distribution or reproduction in other forums is permitted, provided the original author(s) and the copyright owner(s) are credited and that the original publication in this journal is cited, in accordance with accepted academic practice. No use, distribution or reproduction is permitted which does not comply with these terms.

Silver nanoparticles loaded with pomegranate peel extract and hyaluronic acid mediate recovery of cutaneous wounds infected with *Candida albicans*

Marwa I. Abd El-Hamid¹, Doaa Ibrahim ^{2*},
Ahmed Abdelfattah-Hassan^{3,4}, Osama B. Mohammed⁵,
Ioan Pet^{6*}, Samah S. Khalil⁷, Sara M. El-Badry⁸,
Aya Sh. Metwally⁹, Asmaa A. Azouz¹⁰, Ahmed A. Elnegiry¹¹,
Shimaa S. Elnahriry¹², Mirela Ahmadi⁶ and Sara T. Elazab¹³

¹Department of Microbiology, Faculty of Veterinary Medicine, Zagazig University, Zagazig, Egypt,

²Department of Nutrition and Clinical Nutrition, Faculty of Veterinary Medicine, Zagazig University,

Zagazig, Egypt, ³Department of Anatomy and Embryology, Faculty of Veterinary Medicine, Zagazig

University, Zagazig, Egypt, ⁴Biomedical Sciences Program, University of Science and Technology,

Zewail City of Science and Technology, Giza, Egypt, ⁵Department of Zoology, College of Science,

King Saudi University, Riyadh, Saudi Arabia, ⁶Department of Biotechnology, Faculty of Bioengineering

of Animals Resources, University of Life Sciences "King Mihai I" from Timisoara, Timisoara, Romania,

⁷Department of Biochemistry & Molecular Biochemistry, Drug Information Centre, Zagazig University

Hospitals, Zagazig University, Zagazig, Egypt, ⁸Department of Animal Wealth Development, Veterinary

Genetics and Genetic Engineering, Faculty of Veterinary Medicine, Zagazig University, Zagazig, Egypt,

⁹Department of Pharmacology, Faculty of Veterinary Medicine, Aswan University, Aswan, Egypt,

¹⁰Department of Pharmacology, Faculty of Veterinary Medicine, Cairo University, Giza, Egypt,

¹¹Department of Cytology and Histology, Faculty of Veterinary Medicine, Aswan University,

Aswan, Egypt, ¹²Department of Bacteriology, Mycology and Immunology, Faculty of Veterinary

Medicine, University of Sadat City, Sadat City, Egypt, ¹³Department of Pharmacology, Faculty of

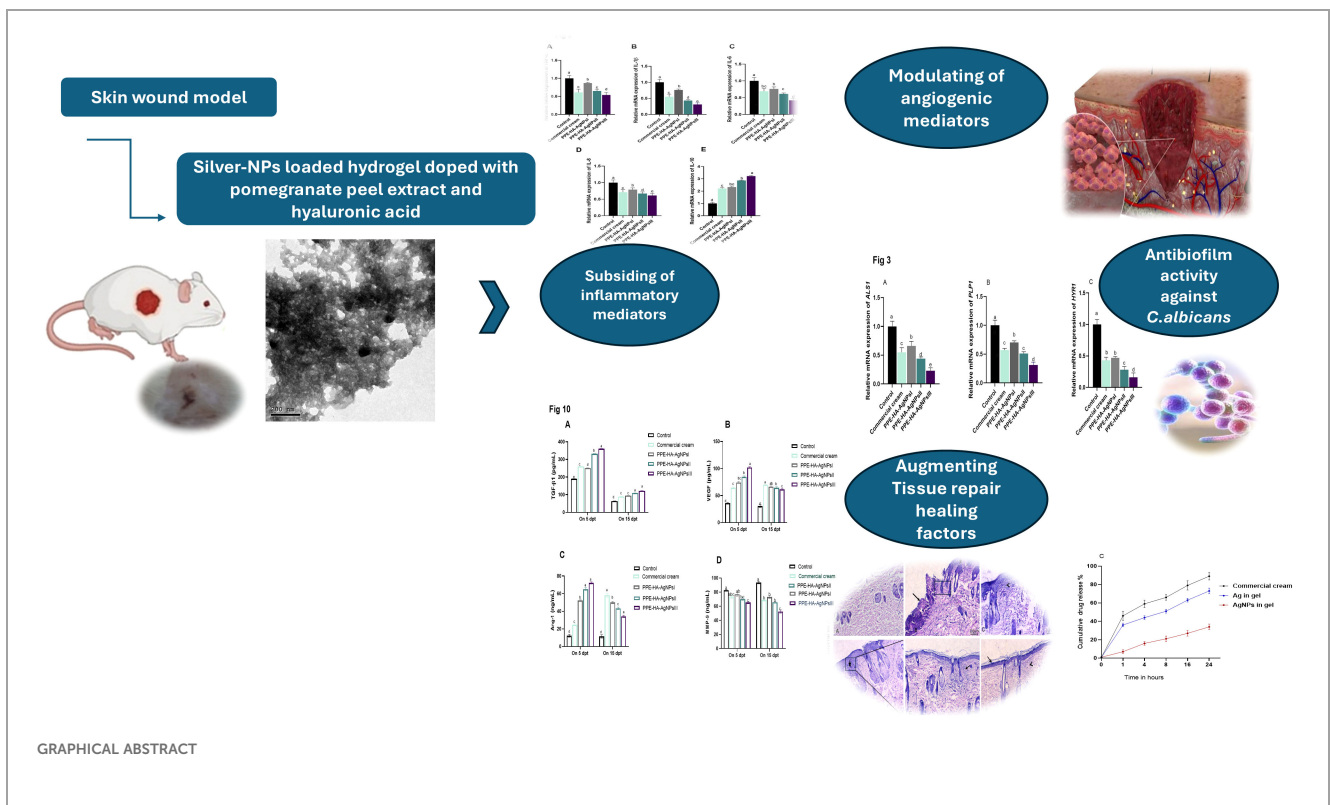
Veterinary Medicine, Mansoura University, Mansoura, Egypt

Smart innovative nanocomposites based on active ingredients and metallic nanoparticles with effective wound healing and antifungal properties are efficient in overcoming the limitations of traditional therapeutic products. Open wounds provide an ideal niche for colonization by *Candida albicans* (*C. albicans*) which poses substantial global health issues owing to delayed wound healing and disordered healing mechanisms. Therefore, proficient innovative therapies that control *C. albicans* infection and promote wound healing are of imperative importance for the management of wounds and prevention of infection and possible complications. This study aims to design a novel nanocarrier platform based on a hydrogel loaded with silver nanoparticles (AgNPs) and doped with pomegranate peel extract (PPE) and hyaluronic acid (HA), offering an unprecedented opportunity to achieve skin repair and manage *C. albicans* colonization with an efficient wound healing process. Sprague-Dawley rats (n=100) were assigned to 5 groups and infected with *C. albicans* and distributed as follows: control positive (untreated) and four cutaneous wound-healing model groups treated topically with commercial cream and PPE-HA-AgNPs at full, 50%, and 25% concentrations for 15 days, respectively. Our findings revealed that the severity of clinical signs, *C. albicans* burden, and the expression of biofilm-related genes *ALS1*, *HYR1*, and *PLB1* were diminished following treatment with PPE-HA-AgNPs. Notably, the formulated

nanocomposite was very effective in extending the release of PPE-HA-AgNPs in infected wounds with retention percentages of 65.4% for PPE-HA-AgNPsIII. Topical administration of PPE-HA-AgNPsIII successfully alleviated the extensive inflammatory response and healed wounded skin via downregulation of tumor necrosis factor-alpha (TNF- α), interleukin-6 and IL-1 beta, and nitric oxide synthase (NOS) levels as shown by enzyme-linked immunosorbent (ELISA) and reverse transcription-quantitative polymerase chain reaction (RT-qPCR) assays. Interestingly, PPE-HA-AgNPsIII modulated angiogenic and wound healing markers as evidenced by the downregulation of MMP-9 and the upregulation of angiopoietin-1 (Ang-1), vascular endothelial growth factor (VEGF) (up to 10 days post-treatment), transforming growth factor-beta 1 (TGF- β 1), *bFGF*, *EGF*, *Ki-67*, and collagen I and III with efficient wound closure capability. This was evidenced by the lessening of histopathological severity, which accelerated the healing of the infected skin wounds post-treatment with PPE-HA-AgNPs. Overall, our formulated PPE-HA-AgNPs provide an effective innovative therapeutic strategy for the treatment of cutaneous wounds infected with *C. albicans* with maximized wound healing efficacy, indicating their potential in clinical practice.

KEYWORDS

Candida albicans, silver nanoparticles, pomegranate peel extract, hyaluronic acid, angiogenesis, wound closure



1 Introduction

The skin provides a natural barrier against the environment and exerts a variety of essential protective functions. Upon disruption of the skin's integrity either by acute injuries or by chronic insults, a multi-step process is initiated, leading to at least a partial reconstruction of the wounded tissue and re-establishment of the skin's barrier function (Okur et al., 2020). Skin wounds are any disruptions or injuries of its anatomical structure and function due to severe breakage. Wound healing remains a significant therapeutic challenge due to the complexity of the healing process. Wound healing is the result of the accumulation of processes including coagulation, inflammation, ground substance and matrix synthesis, angiogenesis, epithelialization, wound contraction, and tissue remodeling (Wang et al., 2018).

Wound infection, whether bacterial or fungal, is often the most common reason for poor wound healing. When a wound becomes infected, the degree of complication is determined by the host's immune competence and the size of bacterial or fungal inoculums. With normal host defenses and adequate debridement, a wound may bear a level of 10^5 pathogenic bacterial species per gram of tissue and still heal successfully (Masoko et al., 2010) but over this number, a wound may become infected. Infections with invasive fungi are still a major cause of worldwide mortality and morbidity, specifically among patients suffering from immune suppression. *Candida albicans* is a major contributor to wound infections and it is considered a global cause of opportunistic mycoses (Gil et al., 2022) with growing economic and medical importance due to extraordinary mortality rates and increased care costs and hospitalization duration (Perween et al., 2019). Moreover, the pathogenicity of *C. albicans* in open wounds is primarily related to a variety of virulence factors that help to form biofilms (Alherz et al., 2022). Up till now, treatment choices have been constrained due to the emergence of resistance to antifungal agents (Perween et al., 2019). On the other hand, various antifungal drug delivery systems to the skin are commercially offered in traditional topical forms such as creams, gels, lotions, ointments, and sprays, resulting in poor penetration (Raina et al., 2023). The problems with these topical forms are their recurrent use for many weeks until the infection signs are relieved and the existence of skin barrier functions, which hinder their delivery and consequently have low efficacy and lead to therapy failure (Firooz et al., 2015). To overcome the aforementioned issues, combining available drugs with modern technology is proposed.

Numerous efforts have been made to design novel agents with long-term efficacy against resistant *C. albicans* and no potential side effects, targeting the healing process in order to avoid the severe complications associated with chronic wounds. In this scenario, applying natural extracts as antifungal drugs is an emergent prospective field that has offered promising and interesting benefits (Nayak et al., 2017). Thus, numerous plant extracts have been investigated for wound treatment, including pomegranate peel extract (PPE), which have wound healing, antimicrobial, antioxidant, and anti-inflammatory functions that are mainly attributed to its phenolic compounds, including flavonoids (anthocyanins, catechins, and other complex flavonoids) and

hydrolyzable tannins (punicalin, pedunculagin, punicalagin, gallic, and ellagic acid) (Ismail et al., 2012). These ingredients have been recognized as the fundamental bioactivity sources accounting for pomegranate's desirable medicinal properties such as its excellent efficacy in dermal wound healing (Lukiswanto et al., 2019).

The use of nanomaterials has emerged as an enormously promising strategy to eradicate infection by virulent fungal, bacterial, and viral species (Aldakheel et al., 2023). There has been widespread employment of metallic nanoparticles to combat human pathogenic microbes in several fields, including pharmaceuticals, medicine, and biology. Metal nanoparticles have excellent antifungal activities via many mechanisms such as ion release, nitrosative and oxidative stress, enzymatic activity inhibition, cell wall and membrane damage, gene expression modulation, and mitochondrial, protein, and DNA dysfunction (Abou Hammad et al., 2020). Silver nanoparticles (AgNPs) have been broadly investigated for their prospective utilization in medicinal fields as antimicrobial agents, drug delivery systems, and nanocarriers (Lázaro-Martínez et al., 2019). AgNPs, in particular, have garnered substantial consideration for their efficacy in suppressing Gram-negative and Gram-positive bacteria, including multidrug-resistant bacterial species (Bruna et al., 2021).

Remarkably, AgNPs can attach to and invade bacterial cell membranes with subsequent destruction and leakage of cellular contents. Likewise, they can hinder essential intracellular functions such as the disruption of the respiratory chain and inhibition of cell division and DNA replication. Furthermore, they also exhibit noteworthy antimicrobial effects against antimicrobial-resistant fungal species by targeting cellular components involved in pathogenicity and drug resistance (Bruna et al., 2021). Recent technological advances in the stability and biocompatibility of AgNPs via surface alterations make them significant candidates for carrying many compounds with antifungal activity (Brown et al., 2013). The use of hydrogel scaffolds can improve the weak binding affinity of the surface of AgNPs. Thus, hydrogels can promote wound healing by maintaining equilibrium between oxygen, hydration, and chemical exchange. Hydrogels' cross-linked three-dimensional assembly and hydrophilic polymer system permit them to play a functional role as water-sustaining scaffolds and provide a stable and efficient environment for AgNP delivery (Aldakheel et al., 2023). In addition, hyaluronic acid (HA), a natural polysaccharide, plays a fundamental role in tissue repair modulation, angiogenesis, cell motility, and signal transduction as it is a major constituent of the extracellular matrix (Dulińska-Litewka et al., 2021).

In the current study, the addition of natural compounds that possess antimicrobial and antioxidant properties to a hydrogel loaded with AgNPs may enhance their effectiveness against *C. albicans* infection, offering unique properties for biomedical applications such as their aptitude to combat fungal resistance, promote antifungal activity against planktonic and biofilm-embedded fungal species, diminish cell toxicity, and the opportunity to lessen the antimicrobial dosage (Skłodowski et al., 2023). We hypothesize that a PPE-HA-AgNP hydrogel will (a) significantly reduce *C. albicans* biofilm formation, (b) enhance wound closure, and (c) promote angiogenesis through the modulation of cytokines and growth factors and may prove to be

an innovative and efficient strategy for the clinical treatment of cutaneous wounds.

2 Materials and methods

2.1 Preparation of pomegranate peel extract

Consistent with the method prescribed in a previous study (de Oliveira et al., 2013), PPE was prepared. Briefly, pomegranate peels were finely ground, dried at 50°C, and then extracted with ethanol (70%). After that, the mixture was left in the dark for 24 h at room temperature, and then purified. The prepared extract was concentrated to dryness, frozen at -70°C for 24 h for lyophilization, and then stored in a light-protected container at -20°C. A high-performance liquid chromatography (HPLC) assay was utilized to estimate the polyphenolic fractions of the prepared PPE, as shown in Table 1.

2.2 Synthesis and characterization of the nanocomposite-loaded hydrogel

The protocols described by Gorup et al. (2011) and Das et al. (2015) were used with modifications to produce AgNPs. Briefly, 20 mL of PPE (30 mg/mL) was mixed with a solution of AgNO₃ (0.01 M, Sigma Aldrich, St Louis, MO, USA) at a pH of 8. The reaction mixture was then left for 20 minutes at room temperature and the nanoparticle solution was centrifuged for 30 minutes at 10,000 rpm and then the collected PPE-HA-AgNP pellets were freeze-dried. The preparation of the hydrogel was carried out in line with (Ruffo et al., 2022) as carboxymethylcellulose (CMC) (Labsynth, Diadema, Brazil) was dissolved in water (2% w/v) and 20% of propylene glycol (Labsynth,

Diadema, Brazil) and the mixture was stirred at room temperature for 30 minutes. Sodium hyaluronate (HA, 95%) of a low molecule weight grade (Shandong Focuschem Biotech Co, Ltda, Jinning, Shandong, China) was homogenized in purified water at 10,000 rpm for 5 min utilizing a rotor-stator (Staufen, Baden-Württemberg, Germany) to a final concentration of 0.01 g/mL. In the next step, CMC and HA were proportionally homogenized (1:1) at 10,000 rpm for 5 min using a rotor-stator (Staufen, Baden-Württemberg, Germany). Subsequently, the PPE-HA-AgNP pellets were added to the previously prepared mixture (0.01% w/w) and stirred at room temperature for 6 h. After that, citric acid was added as a crosslinking agent and the final obtained mixture was incubated at room temperature for a further 6 h. To obtain the final hydrogel loaded with PPE-HA-AgNPs, the prepared solution was freeze-dried and subsequently stored at room temperature for further characterization. The final concentrations of the ingredients in the formulated PPE-HA-AgNP-loaded hydrogel were 0.005, 0.094, and 0.34 g/mL for HA, PPE, and AgNPs, respectively. The average particle size and morphology in the synthesized PPE-HA-AgNP-loaded hydrogel were assessed using transmission electron microscopy (Figure 1A) at the National Centre for Radiation Research and Technology, Egypt. Furthermore, the particle size distribution of the PPE-HA-AgNP-loaded hydrogel (Figure 1B) was performed using dynamic light scattering (Zetasizer Nano ZS, Malvern, UK). The entrapment efficiency (EE%) of the prepared PPE-HA-AgNP-loaded hydrogel was determined according to a previously established method (Shafique et al., 2017).

2.3 *In vitro* release of the formulated therapeutic agents

To determine the *in vitro* release of the used therapeutic agents from the nanocomposite-loaded hydrogel, phosphate-buffered saline (pH=7.4)

TABLE 1 Polyphenolic compounds of pomegranate peel extract analyzed by HPLC assay.

Analyzed extracted fractions (mg/kg)					
Rutin	2.66	Quercetrin	34.11	Vanillic	7.55
Quercetrin-3-O-glucose	1.89	Cinnamic	27.13	Ellagic	121.99
Catechol	60.15	Gallic	25.44	Apegnin	1.35
Hespirtin	5.54	Apigenin-7-glucose	7.05	Catechein	32.90
Quercetin	2.25	Naringin	9.44	Salicylic	1.31
Caffeine	12.88	Kaemp.3-(2-p-coumaroyl) glucose	8.39	Rosmarinic	13.00
Chlorogenic	18.00	p-coumaric	0.69	Acacetin7 neo hesperside	4.33
Coumarin	8.32	Ferulic	3.99	Pyrogallol	298.79
Apig.6-rhamnose galactose	7.50	Acacetin7 neo-hesperside	3.89	Apig.6-arbinose 8-galactose	3.28
Rhamentin	2.90	Benzoic	7.11	3,4,5-methoxycinnamic	1.09
Kaempferol	1.25	Luteo.7-glucose	6.23	Apig.7-O-neohesperidoside	3.15
4-Amino-benzoic	0.66	Protocatchuic	19.22	Alpha-coumaric	3.27
Iso-ferulic	0.79	Caffeic	4.60		

and Tween-20 (2% w/v) were added to the dissolution medium and then the nanocomposite-loaded hydrogel was dispersed in the prepared dissolution medium and magnetically stirred at 37°C (Kataoka et al., 2021). An *in vitro* release assay was performed at different intervals (1, 4, 8, 16, and 24 h, Figure 1C) and the amount of therapeutic agents in the examined samples were analyzed via the established HPLC assay.

2.4 *In vitro* anti-candidal activity of PPE-HA-AgNPs

2.4.1 Fungal *C. albicans* strain and growth condition

A pathogenic clinical *C. albicans* isolate was obtained from a patient with mucocutaneous candidiasis and kept on Sabouraud dextrose agar (SDA, Oxoid, UK) slopes at 4°C. The phenotypical characteristics comprising color and morphology of the isolate were identified on HiCrome Candida differential agar medium (HiMedia, India), with the micromorphological characteristics identified on rice agar with Tween 80 (HiMedia, India), and its ability to produce germ tube was tested with biochemical tests including carbohydrate assimilation and fermentation and urease production (Kurtzman et al., 2011).

2.4.2 Agar well diffusion method

The anti-candidal activity of PPE-HA-AgNPs was estimated using an agar well diffusion assay, in triplicate, as described previously (Patra and Baek, 2017). A sterile *C. albicans* culture was used to prepare a 0.5 McFarland standard suspension in 0.9% sterile saline solution with a final concentration of 10⁸ colony-forming units (CFU)/mL and the prepared fungal inoculum was spread on Sabouraud dextrose agar medium. Using a sterile cork borer, 6-mm wells were made on the surface of the agar medium. The PPE-HA-AgNP solution was prepared by dissolving the pellets in 10% dimethyl sulfoxide (DMSO; Oxoid, UK). Each well was filled with 50 µL of the prepared PPE-HA-AgNP solution which was used as a negative control and fluconazole (5 mg/mL) as a positive control. The inoculated plates were incubated at 37°C for 24 h and the zones of inhibition were then measured in millimeters.

2.4.3 Broth microdilution method

A broth microdilution assay was performed, in triplicate, to determine the minimum inhibitory concentration (MIC) and minimum fungicidal concentration (MFC) of the PPE-HA-AgNPs using sterile 96-well rounded-bottom plates according to Clinical and Laboratory Standards Institute guidelines (CLSI, 2012). Briefly, Mueller–Hinton broth (Oxoid, UK) was dispensed into the

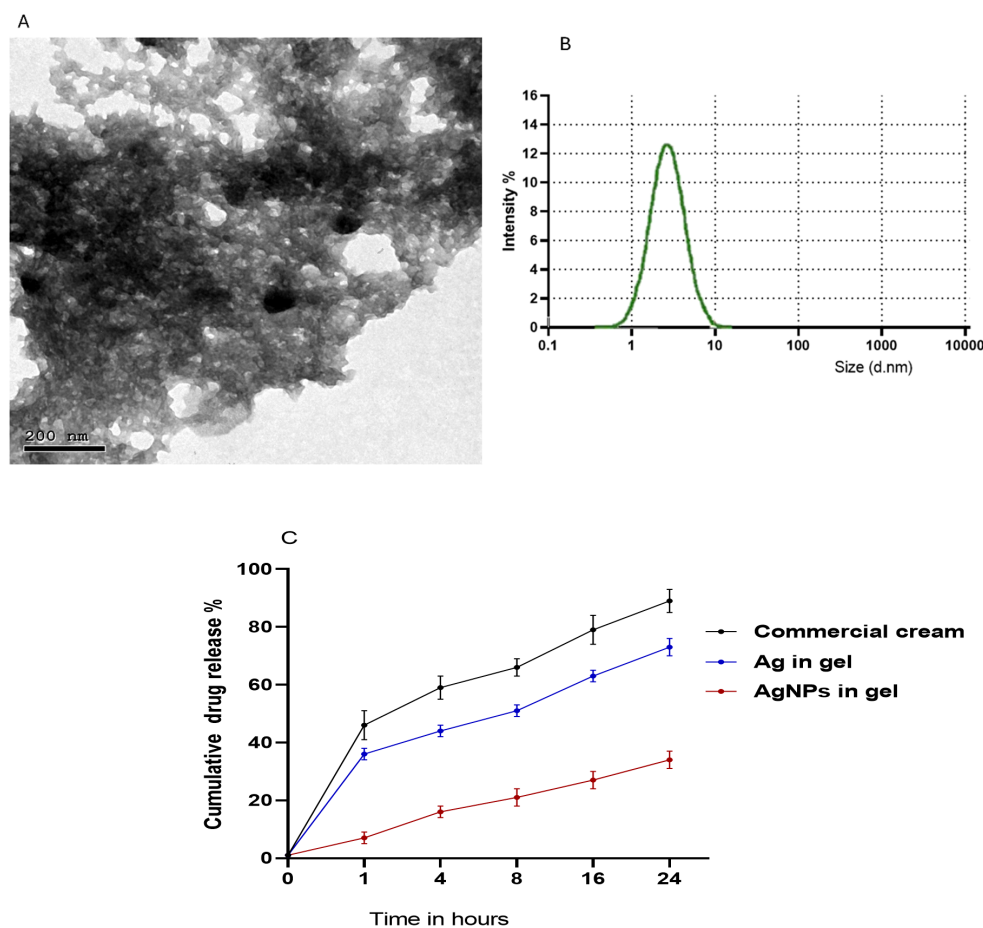


FIGURE 1 Transmission electron microscopy (A), particle size distribution (B), and *in vitro* release of PPE-HA-AgNP-loaded hydrogel (C).

microtiter plate wells and double-fold serial dilutions of PPE-HA-AgNPs with concentrations ranging from 0.625 to 10 µg/mL were made. After that, a fungal suspension prepared in brain heart infusion broth at a concentration of 5×10^5 CFU/mL was added to each dilution. Positive (PPE-AgNP-free broth media containing fungal suspensions) and negative (fungal-free broth medium) control wells were also included. The plate was incubated at 37°C for 24 h and the culture turbidity was visually examined. The lowest concentration of PPE-HA-AgNPs (µg/mL) that had no turbidity (lack of visible fungal growth) was considered the MIC. To determine the MFC of the tested PPE-AgNPs, all fungal growth-free wells were cultured on SDA plates. The inoculated plates were incubated at 37°C for 24 h and subsequently counted to determine the viable CFU/mL. The MFC that induced a fungicidal effect was considered to be the lowest concentration of PPE-HA-AgNPs that showed no visible viable fungal colonies on SDA agar plates.

2.5 *In vivo* wound-healing model

2.5.1 Ethical statement

All animal housing and management protocols were approved by the Zagazig University's Animal Ethics Committee. Ethical approval was attained prior to the commencement of the experimental study and all animal experiments were conducted in conformity with ethics and guidelines of the Institutional Animal Care and Use Committee of the Faculty of Veterinary Medicine, Mansura University, (MU-ACUC).

2.5.2 Experimental animals and housing conditions

In total, 100 healthy male Sprague-Dawley rats (8-10 weeks old) weighing 150-200 g were obtained from the Laboratory Animals unit, Faculty of Veterinary Medicine, Zagazig University, Egypt. They were housed in separate stainless-steel cages at a temperature of $22 \pm 3^\circ\text{C}$ and relative humidity of 55%–65% in a 12 h light/dark cycle. All the rats were maintained under specified pathogen-free conditions and allowed a standard diet and drinking water *ad libitum*. Prior to the beginning of the experiment, the rats were allowed to acclimatize for 2 weeks under standard animal housing conditions.

2.5.3 Preparation of the *C. albicans* strain and induction of fungal infection

The pathogenic clinical *C. albicans* strain cells grown on SDA medium were suspended in sterile saline to attain a target density of approximately 10^7 CFU/mL (Barros et al., 2007). The rats were intradermally injected with 100 µL of the prepared *C. albicans* inoculum. The induced fungal infection was monitored after 3 days of inoculation in the affected skin area.

2.5.4 Wound creation

The dorsal skin of rats was shaved with electrical clippers, and the exposed skin area was sterilized with 70% ethanol and allowed

to dry. The rats were anesthetized with an intramuscular injection of ketamine (50 mg/kg) and xylazine (5 mg/kg). Under aseptic conditions, evenly spaced wounds were created on each animal using sterile 2 mm diameter biopsy punch equipment (Simonsen et al., 2002). Thereafter, the rats were housed individually and observed in disinfected cages to prevent infection or further wound damage.

2.5.5 Experimental design

Rats were randomly allocated into five experimental groups (20 rats/group) in separate cages. After cutaneous wound creation, all rats were infected with the prepared *C. albicans* strain and distributed as follows: the control positive group with rats with untreated infected cutaneous wounds) and four wound-healing model groups with the first group comprising rats with infected cutaneous wounds that were treated with commercially available ketoconazole cream (2%) as a reference drug; the other three groups contained rats with infected cutaneous wounds that were treated with the formulated nanocomposite at three different concentrations: 25% (PPE-HA-AgNPsI), 50% (PPE-HA-AgNPsII), and 100% (PPE-HA-AgNPsIII).

The wounds were cleaned using cotton wool and all treatments were started after verification of the induced wound infection and applied topically every day for 15 days. All the animals were observed daily and examined to check for any clinical symptoms.

2.5.6 Investigation of clinical lesions

The infected skin area was observed periodically to check the clinical parameters and effectiveness of the applied therapeutic agents on the 1st, 4th, and 7th days each week and lesions were graded on a five-point scale (from 0 to 5) (Aggarwal et al., 2013) as follows: 0, no sign of infection; 1, slight erythematous skin; 2, redness on a well-defined area with swelling, bald patches, and scaly area; 3, large areas with redness and ulceration; 4, loss of hair and partial damage to the skin; and 5, excessive damage to the skin with complete hair loss.

2.5.7 Estimation of the penetration efficacy of the used therapeutic agents

The amount of PPE-HA-AgNPs and ketoconazole cream present in the uppermost layer of the skin, stratum corneum, was estimated using the tape-stripping method as employed previously (Luengo et al., 2006). Additionally, the amount of penetrated PPE-HA-AgNPs and ketoconazole cream was determined after washing, cutting, and homogenizing the skin pieces for 2 h, followed by centrifugation for 10 min at 3,000 RCF and HPLC analysis (Minghetti et al., 2006).

2.5.8 Monitoring of wound closure

The progressive decrease in the wound size and wound closure indicated by the formation of new epithelial tissue layers covering the wound were monitored periodically (every 3 days) until the 21st day of the study by tracing the wound boundaries using a transparent paper sheet and a marker. The wound healing degree was calculated as per the following formula:

Wound retraction (%)

$$= (\text{initial wound area} - \text{area of measured wound}) / \text{initial wound}$$

2.5.9 Collection of skin samples

On days 5, 10, and 15 post-treatment, five rats from each group were humanely sacrificed and wound tissue specimens were excised and divided into four pieces. One wound piece was homogenized in Tris buffer saline for further assessment of some biochemical parameters including tumor necrosis factor- α (TNF- α), interleukin (IL)-6, IL-1 beta (IL-1 β) inflammatory cytokines, nitric oxide (NO), nitric oxide synthase (NOS), C-reactive protein (CRP), and myeloperoxidase (MPO). The second wound piece was homogenized in sterile isotonic saline solution and stored at -20°C for subsequent quantitative determination of tissue *C. albicans* burden, the third piece was kept in RNALater (Sigma Aldrich, St Louis, MO, USA) for gene expression analysis, and the last piece was fixed in neutral buffered formalin (10%) for histopathological inspection.

2.5.10 Fungal burden

To assess the fungal burden on days 5, 10, and 15 post-treatment, homogenates of wound tissues were subjected to 10-fold serial dilutions and aliquots of the resultant homogenates were subsequently plated onto SDA plates. After a 48 h incubation of the inoculated SDA plates at 37°C, the number of *C. albicans* colonies was counted on each plate and expressed as CFU/g, and then log₁₀ of the CFU numbers were calculated (Zhang et al., 2021). All SDA plates were carried out in duplicate and the mean fungal counts of the duplicate plates were analyzed and used for later analysis.

2.5.11 Evaluation of inflammatory and wound healing-related biomarkers

All inflammatory markers were estimated on days 5 and 10 post-treatment. Rat wound tissue homogenate samples were diluted and assayed to determine the levels of TNF- α , IL-6, and IL-1 β inflammatory cytokines via specific Thermo Scientific™ rat cytokine enzyme-linked immunosorbent (ELISA) kits (Cat. No. BMS622, BMS625 and BMS630, respectively). The levels of NO and NOS in the wound tissue homogenates were also estimated by colorimetric assays using QuantiChrom™ Nitric Oxide and EnzyChrom™ Nitric Oxide synthase kits, respectively. Moreover, CRP levels were measured using a commercial kit (AG723-M, Sigma-Aldrich, USA) and MPO activity was determined via an ELISA kit (E4581-100, BioVision, CA, USA). All procedures were carried out according to the manufacturer's guidelines. Moreover, ELISA assays were utilized to estimate the concentrations of transforming growth factor-beta 1 (TGF- β 1) (MultiSciences, Biotech, Co., Hangzhou, China), vascular endothelial growth factor (VEGF) (Abcam, Cambridge, USA), angiopoietin-1 (Ang-1) (Elabscience, USA) and matrix metalloproteinase-9 (MMP-9) (Elabscience, USA) on days 5 and 15 post-treatment.

2.5.12 Assessment of total antioxidant capacity and lipid peroxide concentration

On day 10 post-treatment, the skin tissue homogenates were used to estimate the levels of lipid peroxides reflected by malondialdehyde

(MDA) via a specific commercial colorimetric kit (Cat. No. LIP39-K01) purchased from Eagle Biosciences, Inc. (Boston, USA) and total antioxidant capacity (TAC) was calculated via a Cayman TAC assay kit (Cayman Chemical Co., Ann Arbor, USA) following manufacturer's instructions. Furthermore, ELISA kits (MyBioSource; San Diego, USA) were utilized for the measurement of glutathione peroxidase (GSH-Px), catalase (CAT), and superoxide dismutase (SOD) activity (Cat. No. MBS028183, MBS006963 and MBS036924 respectively) according to manufacturer's protocols. Reactive oxygen species (ROS) content in the skin tissues was determined using a specialized ELISA kit (Cat. No. MBS039665, MyBioSource; San Diego, USA) according to the manufacturer's instructions. Moreover, hydrogen peroxide (H₂O₂) levels were estimated using methods detailed previously (Loreto and Velikova, 2001) and their amounts were expressed as $\mu\text{mol/g}$ of skin tissue.

2.5.13 Quantification analysis using reverse transcription-quantitative polymerase chain reaction assays

Quantitative transcriptional analysis was utilized to investigate the effect of the PPE-HA-AgNPs on genes encoding inflammatory mediators, i.e., TNF- α , IL-6, IL-18, IL-1 β , and IL-10, on day 5 post-treatment; on antioxidant markers, i.e., glutathione peroxidase (GSH-Px), CAT, SOD, heme oxygenase-1 (HO-1), NAD(P)H quinone oxidoreductase 1 (NQO1), and nuclear factor erythroid 2-related factor 2 (Nrf2) on day 10 post-treatment; on angiogenic and wound healing markers, i.e., matrix metalloproteinase-9 (MMP-9), collagen I and III, VEGF, Ang-1, TGF- β 1, basic fibroblast growth factor (bFGF), epidermal growth factor (EGF), and antigen Kiel-67 (*Ki-67*) on days 5, 10, and 15 post-treatment; and on *C. albicans* agglutinin-like sequence 1 (*ALS1*), hyphally regulated (*HYR1*), and phospholipase B (*PLB1*) genes on day 15 post-treatment. Total *C. albicans* RNA was extracted according to the technique described in the RNeasy Mini kit (Qiagen, Germany) and then a one-step reverse transcription-quantitative polymerase chain reaction (RT-qPCR) procedure was utilized for all mRNA quantifications via a QuantiTect SYBR Green RT-PCR kit (Qiagen, Germany) on the Stratagene MX3005P (Agilent Technologies, Santa Clara, CA, USA) real-time PCR thermal cycler. All PCR reactions were conducted in three independent replicates. Melting curve analysis was subsequently carried out to confirm the presence of specific amplicons. A list of primer sets used in all RT-qPCR assays for the gene expression analyses is given in Table 2. The expression of *C. albicans* biofilm-associated genes was normalized against the elongation factor 1-beta (*EFB1*) housekeeping gene. Furthermore, β -actin was utilized as an internal reference gene for normalizing the expression levels of the other inflammatory, antioxidant, angiogenic, and wound healing-associated genes. The relative fold changes in target gene expression were determined using the comparative Ct method, referred to as 2^{- $\Delta\Delta\text{Ct}$} (Livak and Schmittgen, 2001).

2.5.14 Histopathological analysis

On days 5 and 15 post-treatment, the rat skin tissues in all the experimental groups were fixed in neutral buffered formalin solution (10%) for 24 h, and then dehydrated in grade ethanol, cleaned in xylene, embedded in paraffin, and cut using a Leica

TABLE 2 Primer sequences utilized for gene expression analysis via RT-qPCR assays.

Specificity/Target gene	Primer sequence (5'-3')	Accession No./Reference
Inflammatory mediators		
<i>IL-1β</i>	F: TGACAGACCCCAAAAGATTAAGG R: CTCATCTGGACAGCCCAAGTC	NM_031512.2
<i>IL-6</i>	F: CCACCAGGAACGAAAGTCAAC R: TTGCGGAGAGAAACTTCATAGCT	NM_012589.2
<i>IL-18</i>	F: ATGGCTGCCATGTCAGAAAGA R: TTGTTAAGCTTATAAATCATGCGGCCTCAGG	XM_039080945.1
<i>IL-10</i>	F: GCCCAGAAATCAAGGAGCATT R: CAGCTGTATCCAGAGGGTCTTCA	L02926.1
<i>TNFα</i>	F: CAGCCGATTGCCATTCA R: AGGGCTCTTGATGGCAGAGA	L19123.1
Antioxidant markers		
<i>CAT</i>	F: ACGAGATGGCACACTTTGACAG R: TGGGTTTCTTCTTGCTATGG	NM_012520.2
<i>SOD</i>	F: AGCTGCACCACAGCAAGCAC R: TCCACCACCTTAGGGCTCA	NM_017051.2
<i>GSH-Px</i>	F: AAGGTGCTGCTCATTGAGAATG R: CGTCTGGACCTACCAGGAACT	NM_030826.4
<i>HO-1</i>	F: CCCAGAGGCTGTGAACCTCTG R - AGGCCCAAGAAAAGAGAGCC	NM_012580.2
<i>Nrf2</i>	F: GGTGCCCACATTCCCAAAC R - GGCTGGGAATATCCAGGGCA	NM_031789.2
<i>NQO1</i>	F: CATTCTGAAAGGCTGGTTGA R: CTAGCTTTGATCTGGTTGTCAG	(Yeligar et al., 2010)
Angiogenic and wound healing markers		
<i>TGF-β1</i>	F: CCAGCCGCGGGACTCT R: TTCCGTTTACCAGCTCCAT	NM_021578.2
<i>VEGF</i>	F: GATCCAGTACCCGAGCAGTCA R: TCTCCTTCTTTTTGGTCTGCAT	NM_053549.1
<i>Ang-1</i>	F: AGGTGGTGGTTTGATGCCT R: CGGGAACATCCCCAGATTGT	NM_017232
<i>MMP-9</i>	F: GACACCACCGAGCTATCCAC R: TTAAACGGGCTGTTCCCT	(Zhao et al., 2023)
Collagen I	F: TTTGGAGAGAGCATGACCGA R: AGGGACTTCTTGAGGTTGCC	(Zhao et al., 2023)
Collagen III	F: TGCAATGTGGACCTGGTTT R: GGGCAGTCTAGTGGCTCATC	(Zhao et al., 2023)
<i>Ki-67</i>	F: GGGTTTCCAGACACCAGACC R: CCAGGAAGACCAGTTAGAACC	NM_001271366.1
<i>EGF</i>	F: CTCAGGCCTCTGACTCCGAA R: ATGCCGACGAGTCTGAGTTG	NM_012842.1
<i>bFGF</i>	F: CGATAGAACACGGCATCAaTC R: CATCAGGCAGTTCGTAGCTC	NM_019305.2
<i>C. albicans</i> biofilm		
<i>ALS1</i>	F: CCATCACTGAAGATATCACCACA R: TGGAGCTTCTGTAGGACTGGTT	(Cheng et al., 2005)
<i>HYR1</i>	F: TTGTTTGGGTCATCAAGACTTTG R: GTCTTCATCAGCAGTAACACAACCA	(Tsang et al., 2012)

(Continued)

TABLE 2 Continued

Specificity/Target gene	Primer sequence (5'-3')	Accession No./Reference
<i>C. albicans</i> biofilm		
<i>PLB1</i>	F: GGTGGAGAAGATGGCCAAAA R: AGCACTTACGTTACGATGCAACA	(Nailis et al., 2010)
Housekeeping genes		
β -actin	F: CGCAGTTGGTTGGAGCAAA R: ACAATCAAAGTCTCAGCCACAT	V01217.1
<i>EFB1</i>	F: TCAGATTCTCTAAAGTCG R: TGACATCAGCTTGAGTGG	X96517

IL, interleukin; *TNF- α* , tumor necrosis factor-alpha; *CAT*, catalase; *SOD*, superoxide dismutase; *GSH-Px*, glutathione peroxidase; *HO-1*, heme oxygenase-1; *Nrf2*, nuclear factor erythroid 2-related factor 2; *NQO1*, NAD(P)H quinone oxidoreductase 1; *TGF- β 1*, transforming growth factor beta 1; *VEGF*, vascular endothelial growth factor; *Ang-1*, angiopoietin-1; *MMP-9*, matrix metalloproteinase-9; *Ki-67*, Kiel-67; *EGF*, epidermal growth factor; *bFGF*, basic fibroblast growth factor; *ALSI*, *C. albicans* agglutinin-like sequence 1; *HYR1*, hyphally regulated gene; *PLB1*, phospholipase B; *EFB1*, elongation factor 1-beta.

microtome. After that, prepared skin tissue sections (5- μ m) were subjected to staining with hematoxylin and eosin (H&E) and examined under light microscopy (Bancroft and Gamble, 2008).

2.6 Statistical analysis

Statistical assessment of all measured parameters was performed using one-way analysis of variance (ANOVA) via SPSS statistical software version 20 (IBM Corp., USA SPSS[®] program version 22 (SPSS Inc., Chicago, IL, USA) with a sample size of n=5/group. Validating the statistical methods was done via homogeneity and variance normality using Levene and Shapiro-Wilk tests, respectively. Variations among the studied experimental groups were examined using Tukey's *post-hoc* test. All data were presented as means \pm standard errors with statistically significant values at $p < 0.05$. All the graphs were created using GraphPad Prism (Version 8, GraphPad Software Inc.). The fold change was assessed by the following equation: (B-A)/A, where the least value is A and the maximum value is B. Relative fold changes in the expression of specific genes were calculated by the $2^{-\Delta\Delta C_t}$ method (Livak and Schmittgen, 2001).

3 Results

3.1 *In vitro* anti-candidal activity of the PPE-HA-AgNPs

Regarding the susceptibility of the *C. albicans* strain to the PPE-HA-AgNPs, the investigated strain was highly susceptible to the formulated nanocomposite, with a recorded inhibition zone diameter of 34 mm as estimated via an agar well diffusion assay and the corresponding MIC and MFC values of 1.25 and 2.5 μ g/mL, respectively, as determined by the broth microdilution method.

3.2 Clinical observation

The efficacy of the PPE-HA-AgNP-loaded hydrogel on lesion severity was described and scored accordingly, as shown in Table 3.

It was observed that the infected and untreated rats displayed no signs of improvement with clinical findings of excessive hair loss, redness, and damage to the skin. Furthermore, the group treated with PPE-HA-AgNPsI showed little improvement with moderate areas of redness and ulceration and at the end of treatment period, the infected area in this group was not completely cured. The traditionally and PPE-HA-AgNPsII-treated groups showed slight redness in the defined areas with mild swelling, bald patches, and scaly areas. However, treatment with the PPE-HA-AgNPs at full concentration achieved the maximum curing capability for *C. albicans* infection compared with other treated groups.

3.3 Fungal burden and expression of *C. albicans* biofilm-associated genes

In relation to the outcomes of quantitative analysis of *C. albicans* in skin tissues, lower *C. albicans* populations were found in all the PPE-HA-AgNP-treated groups in a dose-dependent

TABLE 3 Effect of PPE-HA-AgNP-loaded hydrogel at different concentrations on lesion severity.

Group	Lesion	Score
Control	Excessive damage to the skin with complete hair loss	5
Commercial cream	Slight redness, mild swelling, bald patches, and scaly areas	2
PPE-HA-AgNPsI	Large areas with redness and ulceration	3
PPE-HA-AgNPsII	Redness on a well-defined area with swelling, bald patches, and scaly areas	2
PPE-HA-AgNPsIII	Slightly erythematous skin	1

Control: the rats in this group had an experimental cutaneous wound with subsequent *C. albicans* strain infection and received no treatment; commercial cream: rats in this group had an experimental cutaneous wound with subsequent *C. albicans* infection and received a commercially available ketoconazole cream (2%) as a reference drug; PPE-HA-AgNPsI: the rats in this group had an experimental cutaneous wound with subsequent *C. albicans* infection and received a PPE-HA-AgNP formulated nanocomposite at 25% concentration; PPE-HA-AgNPsII: the rats in this group had an experimental cutaneous wound with subsequent *C. albicans* infection and received a PPE-HA-AgNP formulated nanocomposite at 50% concentration; PPE-HA-AgNPsIII: the rats in this group had an experimental cutaneous wound with subsequent *C. albicans* infection and received a PPE-HA-AgNP formulated nanocomposite at full concentration.

manner compared to the control untreated group and these counts steadily diminished over time. Notably, significantly lower ($p < 0.05$) *C. albicans* populations were detected in the skin tissues of the rats treated with PPE-HA-AgNPsIII compared with the control untreated group (Figure 2). The most relevant finding was reported post-treatment with PPE-HA-AgNPsIII, where it was found to have significantly reduced *C. albicans* counts by 2.95 \log_{10} CFU/g on day 15 following treatment.

The relative mRNA expression of *C. albicans* biofilm-related genes tended to be downregulated on day 15 after treatment with PPE-HA-AgNPs in a dose-dependent manner when compared to the control untreated group (Figure 3). Notably, lower expression levels of the *ALS1* gene were observed in the group treated with PPE-HA-AgNPsIII (0.23-fold change), followed by the PPE-HA-AgNPsII group (0.44-fold change). Moreover, the *HYR1* gene was downregulated in these groups (0.16 and 0.28-fold changes, respectively). Furthermore, PPE-HA-AgNPsIII, PPE-HA-AgNPsII, and the topical treatment led to downregulation of the *PLB1* gene (0.31, 0.51, and 0.57-fold changes, respectively) unlike the control untreated group. The most pronounced reduction ($p < 0.05$) in *ALS1*, *HYR1*, and *PLB1* expression levels was detected in the skin tissues of the rats treated with PPE-HA-AgNPsIII (0.23, 0.16, and 0.31-fold changes, respectively).

3.4 Penetration and retention efficacy of the PPE-HA-AgNPs

As shown in Figure 4, a small amount of the commercial cream (358 $\mu\text{g}/\text{cm}^2$, 31.87%) was retained on the skin surface of

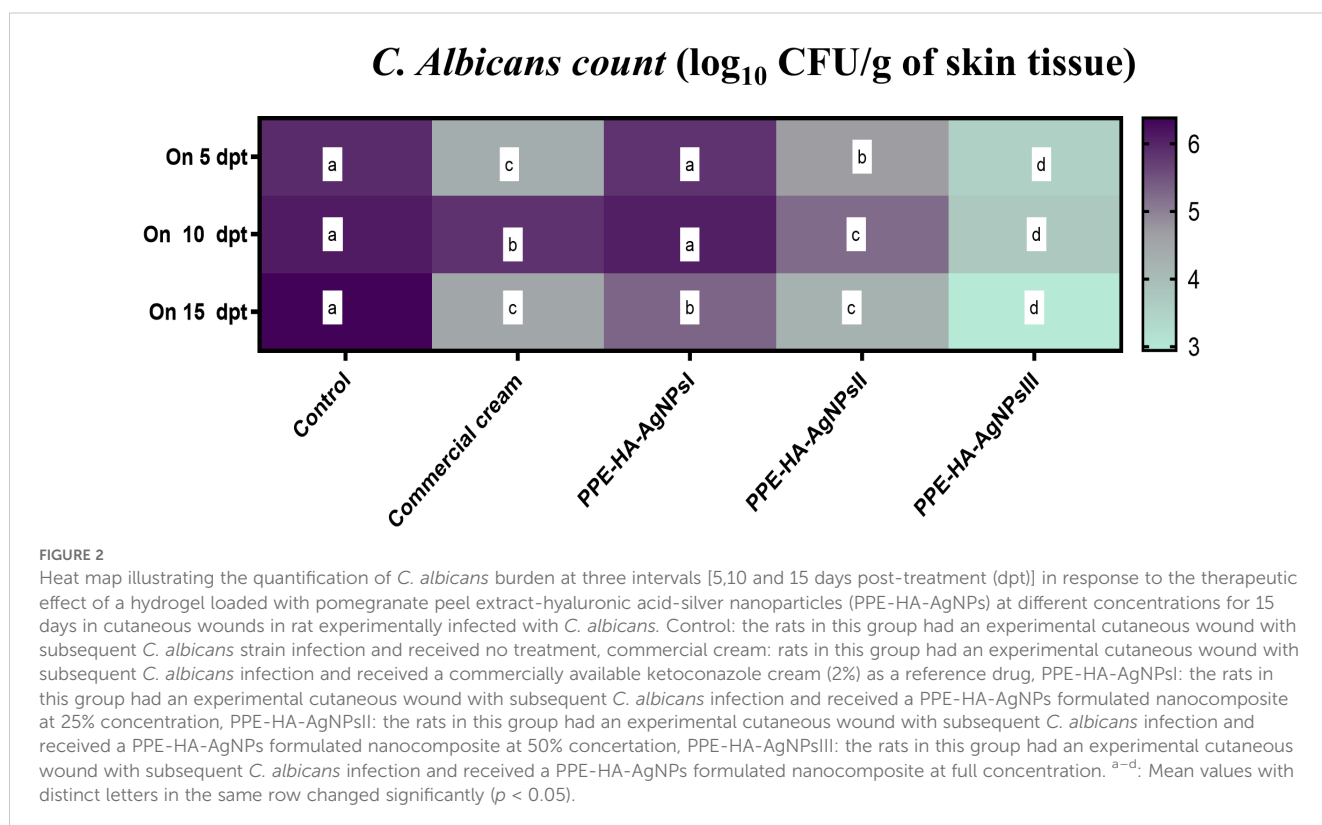
rats after its topical application. Remarkably, the full concentration of PPE-HA-AgNPs showed more retention on the skin surface (713 $\mu\text{g}/\text{cm}^2$, 65.4%) compared with the other concentrations (PPE-HA-AgNPsII: 698 $\mu\text{g}/\text{cm}^2$, 61.2%; and PPE-HA-AgNPsI: 624 $\mu\text{g}/\text{cm}^2$, 56.7%). Moreover, the retention analysis performed to evaluate the amount of therapeutic agent retained in the skin after 24 h demonstrated that the penetration of the commercial cream was much higher (68.12%) than PPE-HA-AgNPsIII (34.52%).

3.5 Wound closure as an endpoint of PPE-HA-AgNP treatment efficacy

As illustrated in Figure 5, the group treated with PPE-HA-AgNPsIII displayed significant ($p < 0.05$) wound retraction compared to the other treated groups at all the investigated intervals. Moreover, the wound closure rate in the PPE-HA-AgNPsIII-treated group on day 21 of the study was over 85%, while that in the groups treated with PPE-HA-AgNPsII and the commercial cream was 80% and 79%, respectively.

3.6 Investigating the healing and therapeutic impact of PPE-HA-AgNPs on inflammatory markers

The effect of the PPE-HA-AgNP-loaded hydrogel on the inflammatory markers, measured using ELISA assays, is shown in Table 4. Notably, TNF- α and IL-6 levels were significantly



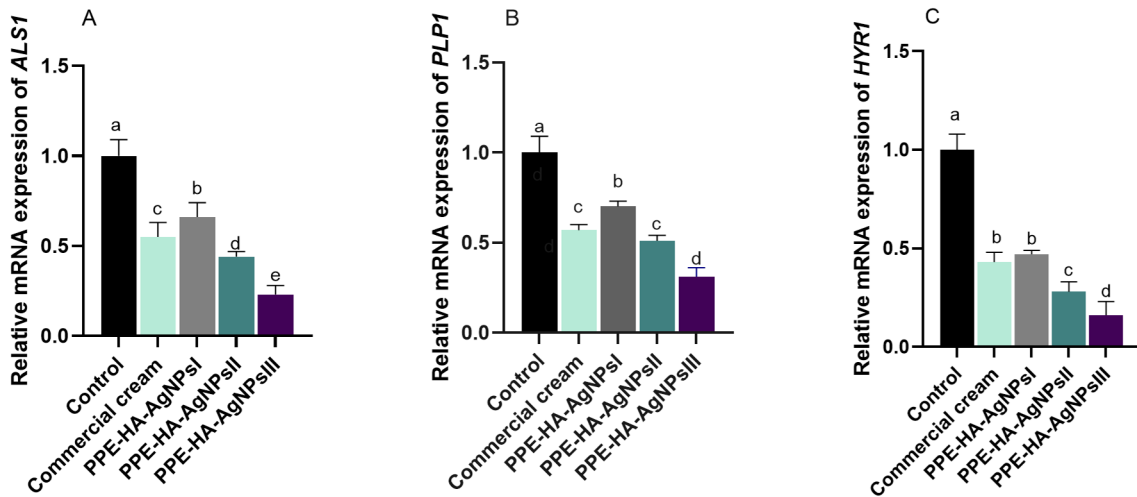


FIGURE 3 Relative mRNA expression of *C. albicans* *ALS1* [agglutinin-like sequence 1, (A)], *PLP1* [phospholipase B, (B)], and *HYR1* [hyphally regulated, (C)] biofilm-related genes on day 15 post-treatment in response to therapeutic efficacy of hydrogel loaded with pomegranate peel extract-hyaluronic acid-silver nanoparticles (PPE-HA-AgNPs) by different concentrations for 15 days in rat cutaneous wound experimentally infected with *C. albicans*. Control: *C. albicans* infected and non-treated rats, commercial cream: ketoconazole cream (2%), PPE-HA-AgNPsl: 25% concentration of formulated nanocomposite, PPE-HA-AgNPslII: 50% concentration of formulated nanocomposite, PPE-HA-AgNPslIII: full concentration of formulated nanocomposite. ^{a-e}Mean values with distinct letters in the same column changed significantly ($p < 0.05$).

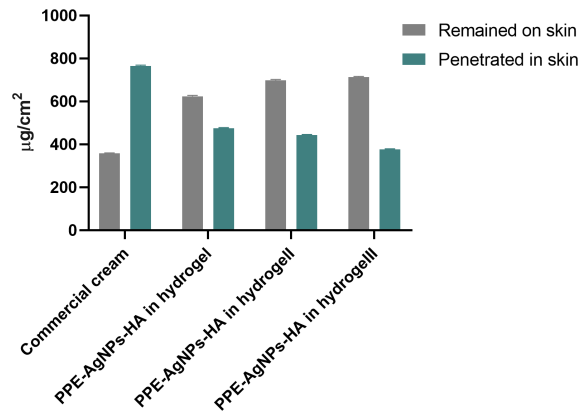


FIGURE 4 Effects of therapeutic concentrations of pomegranate peel extract-hyaluronic acid-silver nanoparticles (PPE-HA-AgNPs) on cutaneous wounds in experimental rats. Commercial cream: ketoconazole cream (2%), PPE-HA-AgNPsl: 25% concentration of the formulated nanocomposite, PPE-HA-AgNPslII: 50% concentration of the formulated nanocomposite, PPE-HA-AgNPslIII: full concentration of the formulated nanocomposite.

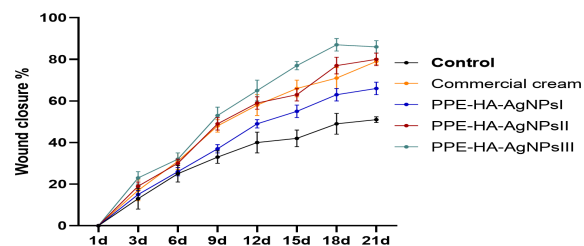


FIGURE 5 The percentage of wound closure measured at 1, 3, 6, 9, 12, 15, 18, and 21 days after wound creation. Commercial cream: ketoconazole cream (2%), PPE-HA-AgNPsl: 25% concentration of the formulated nanocomposite, PPE-HA-AgNPslII: 50% concentration of the formulated nanocomposite, PPE-HA-AgNPslIII: full concentration of the formulated nanocomposite.

TABLE 4 Inflammatory markers in response to therapeutic effects of a hydrogel loaded with pomegranate peel extract-hyaluronic acid-silver nanoparticles at different concentrations in cutaneous wounds in rats experimentally infected with *C. albicans*.

Parameter	Experimental groups					P value	SEM
	On 5 dpt	Control	Commercial cream	PPE-HA-AgNPsI	PPE-HA-AgNPsII		
TNF- α , pg/ μ L	327.33 ^a	171.67 ^c	212.33 ^b	173.00 ^c	153.08 ^d	0.02	1.2
IL-6, pg/ μ L	179.10 ^a	159.00 ^b	137.07 ^c	97.67 ^d	71.87 ^e	< 0.001	1.2
IL-1 β , pg/ μ L	194.00 ^a	131.00 ^c	149.00 ^b	133.33 ^c	127.33 ^c	0.02	2.6
NO (μ mol/ L)	4.93 ^a	4.83 ^a	3.80 ^b	3.10 ^c	2.77 ^c	< 0.001	0.06
NOS (μ mol/ L)	1.87 ^a	1.46 ^{ab}	1.40 ^{ab}	1.37 ^{ab}	1.20 ^b	0.04	0.05
CRP (mg/ L)	14.50 ^a	11.33 ^{ab}	11.43 ^{ab}	8.57 ^{bc}	6.90 ^c	0.001	0.23
MPO (μ mol/L)	12.53 ^d	37.00 ^b	32.23 ^c	44.57 ^a	45.53 ^a	< 0.001	0.34
On 10 dpt							
TNF- α , pg/ μ L	374.33 ^a	138.00 ^c	164.00 ^b	128.00 ^c	109.97 ^d	0.03	3.2
IL-6, pg/ μ L	202.77 ^a	147.00 ^b	125.33 ^c	95.90 ^d	70.50 ^e	< 0.001	1.8
IL-1 β , pg/ μ L	241.00 ^a	131.67 ^b	134.00 ^b	121.33 ^{bc}	110.67 ^c	0.01	2.7
NO (μ mol/ L)	4.17 ^a	3.57 ^{ab}	3.23 ^{bc}	2.77 ^{cd}	2.30 ^d	< 0.001	0.1
NOS (μ mol/ L)	1.47 ^a	1.33 ^{ab}	1.10 ^{ab}	1.10 ^{ab}	0.9 ^b	0.03	0.04
CRP (mg/ L)	16.80 ^a	8.97 ^b	9.43 ^b	6.77 ^b	3.37 ^c	< 0.001	0.17
MPO (μ mol/L)	9.03 ^c	31.33 ^a	27.83 ^b	34.27 ^a	33.50 ^a	< 0.001	0.15

dpt, days post-treatment; TNF- α , tumor necrosis factor-alpha; IL-6, interleukin-6; IL-1 β , interleukin-1 beta; NO, nitric oxide; NOS, nitric oxide synthase; CRP, C-reactive protein; MPO, myeloperoxidase. Control: the rats in this group had an experimental cutaneous wound with subsequent *C. albicans* strain infection and received no treatment, commercial cream: rats in this group had an experimental cutaneous wound with subsequent *C. albicans* infection and received a commercially available ketoconazole cream (2%) as a reference drug, PPE-HA-AgNPs: the rats in this group had an experimental cutaneous wound with subsequent *C. albicans* infection and received a PPE-HA-AgNP formulated nanocomposite at 25% concentration, PPE-HA-AgNPsII: the rats in this group had an experimental cutaneous wound with subsequent *C. albicans* infection and received a PPE-HA-AgNP formulated nanocomposite at 50% concentration, PPE-HA-AgNPsIII: the rats in this group had an experimental cutaneous wound with subsequent *C. albicans* infection and received a PPE-HA-AgNP formulated nanocomposite at full concentration. ^{a-e}Mean values with distinct letters in the same row changed significantly ($p < 0.05$).

decreased following treatment with PPE-HA-AgNPs, in a dose-dependent manner, unlike the ketoconazole cream-treated group, especially on day 10 after treatment. On day 5 following treatment, IL-1 β level revealed no significant variations ($p > 0.05$) among the ketoconazole cream, PPE-HA-AgNPsII, and PPE-HA-AgNPsIII-treated groups; meanwhile, the most significant reduction in IL-1 β level was detected in the PPE-HA-AgNPsIII-treated group on day 10 after treatment.

On day 5 post-treatment, NOS levels did not vary significantly ($p > 0.05$) among all the treated groups, while CRP and NO levels were significantly ($p < 0.05$) lower in PPE-HA-AgNPsII and PPE-HA-AgNPsIII groups, followed by the ketoconazole cream-treated group, compared to the control untreated group. On day 10 after treatment, NO, NOS, and CRP activity in the wound tissues were significantly ($p < 0.05$) diminished in the group treated with the higher concentration of PPE-HA-AgNPs compared with the ketoconazole cream-treated group. On days 5 and 10 following treatment, the PPE-HA-AgNPsII and PPE-HA-AgNPsIII-treated groups exhibited lower MPO in wound tissues compared with the other two (ketoconazole cream and PPE-HA-AgNPsI) treated groups.

Regarding the quantitative evaluation of inflammatory markers by RT-qPCR assays on day 5 after treatment (Figure 6), TNF- α levels were significantly ($p < 0.05$) downregulated in the PPE-HA-

AgNPsIII group, followed by the ketoconazole cream and PPE-HA-AgNPsII-treated groups compared with the control untreated group. Notably, the expression levels of the IL-6, IL-18, and IL-1 β genes in the rats following topical treatment with the PPE-HA-AgNPs were dose-dependent, where the full concentration of PPE-HA-AgNPs caused significant ($p < 0.05$) reductions in their expression (0.42, 0.61 and 0.31-fold changes, respectively). Inversely, treatment with PPE-HA-AgNPs at the higher concentration caused an increase in IL-10 expression (3.22-fold change) compared with the control untreated group.

3.7 Investigating the healing and therapeutic impact of PPE-HA-AgNPs on oxidative and antioxidant-related markers

As illustrated in Figure 7, the group treated with PPE-HA-AgNPsIII, followed by PPE-HA-AgNPsII and then the PPE-HA-AgNPsI-treated groups, presented higher antioxidant enzyme activity unlike the topically treated one. The levels of CAT, SOD, and GSH-Px were significantly increased ($p < 0.05$) in the PPE-HA-AgNPsIII-treated group compared with the control group. Additionally, the skin tissue of the rats treated with PPE-HA-AgNPs at various concentrations had higher TAC and lower

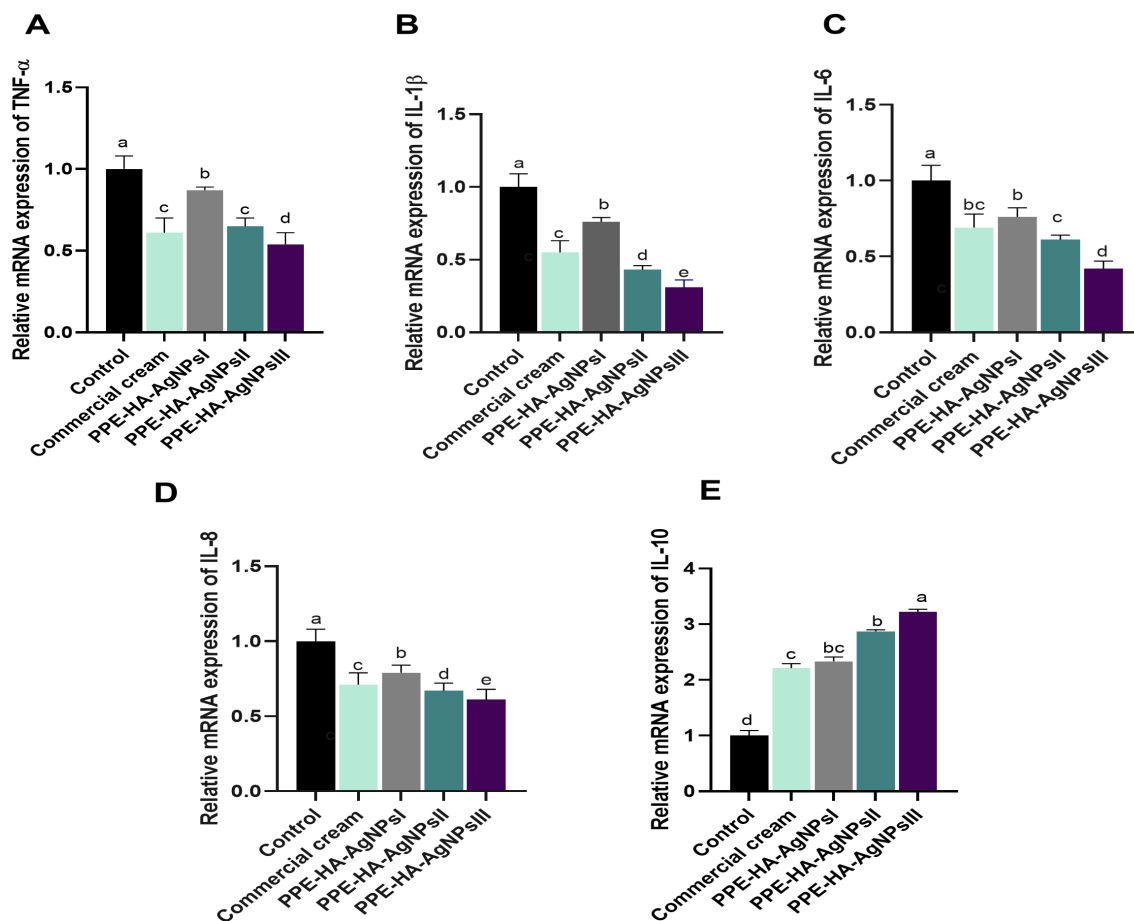


FIGURE 6

Relative mRNA expression of genes encoding cytokines' mediators: *TNF- α* , tumor necrosis factor-alpha (A); *IL-1 β* , interleukin-1 beta (B); *IL-6*, interleukin-6 (C); *IL-18*, interleukin-8 (D); and *IL-10*, interleukin-10 (E) on day 5 post-treatment in response to the therapeutic effect of a hydrogel loaded with pomegranate peel extract-hyaluronic acid-silver nanoparticles (PPE-HA-AgNPs) at different concentrations for 15 days in cutaneous wounds in rats experimentally infected with *C. albicans*. Control: *C. albicans* infected and non-treated rats, commercial cream: ketoconazole cream (2%), PEE-HA-AgNPsI: 25% concentration of the formulated nanocomposite, PPE-HA-AgNPsII: 50% concentration of the formulated nanocomposite, PPE-HA-AgNPsIII: full concentration of the formulated nanocomposite. ^{a-e}Mean values with distinct letters in the same column changed significantly ($p < 0.05$).

MDA contents compared with the control untreated rats. Furthermore, the control untreated group had higher contents of ROS and H_2O_2 compared with the groups treated with PPE-HA-AgNPsII and PPE-HA-AgNPsIII ($p < 0.05$).

The impact of PPE-HA-AgNPs at different concentrations on the molecular mechanisms involved in oxidative and antioxidant status is shown in Figure 8. The expression level of the *NQO1* gene was significantly increased ($p < 0.05$) in the PPE-HA-AgNPsIII-treated group compared with the control group. All the groups treated with PPE-HA-AgNPs at different concentrations showed higher expression levels ($p < 0.05$) of antioxidant-related genes (*CAT*, *SOD*, *GSH-Px*, *HO-1*, and *NQO1*) with simultaneous lower expression levels ($p < 0.05$) of the *Nrf2* gene. The relative mRNA expression of *CAT*, *GSH-Px*, *HO-1*, and *NQO1* reached their peaks ($p < 0.05$) in the group treated with PPE-HA-AgNPsIII (1.56, 1.67, 1.52, and 1.87-fold changes, respectively) in comparison with the control untreated group. In contrast, the groups treated with PPE-

HA-AgNPsII and PPE-HA-AgNPsIII exhibited lower expression levels ($p < 0.05$) of the *Nrf2* gene (0.43 and 0.41-fold change, respectively) in comparison with control untreated group.

3.8 Investigating the healing and therapeutic impact of PPE-HA-AgNPs on angiogenic and wound healing markers

On day 5, the *MMP-9* expression level was significantly ($p < 0.05$) decreased in all the topically treated groups compared with the control untreated group and it gradually decreased over time, especially in the PPE-HA-AgNPsII and PPE-HA-AgNPsIII-treated groups. Notably, the PPE-HA-AgNPsIII-treated group expressed higher levels of both collagen I and III on days 5 and 10 post-treatment. Meanwhile, on day 15 after-treatment, the groups treated with PPE-HA-AgNPsII, PPE-HA-AgNPsIII, and ketoconazole

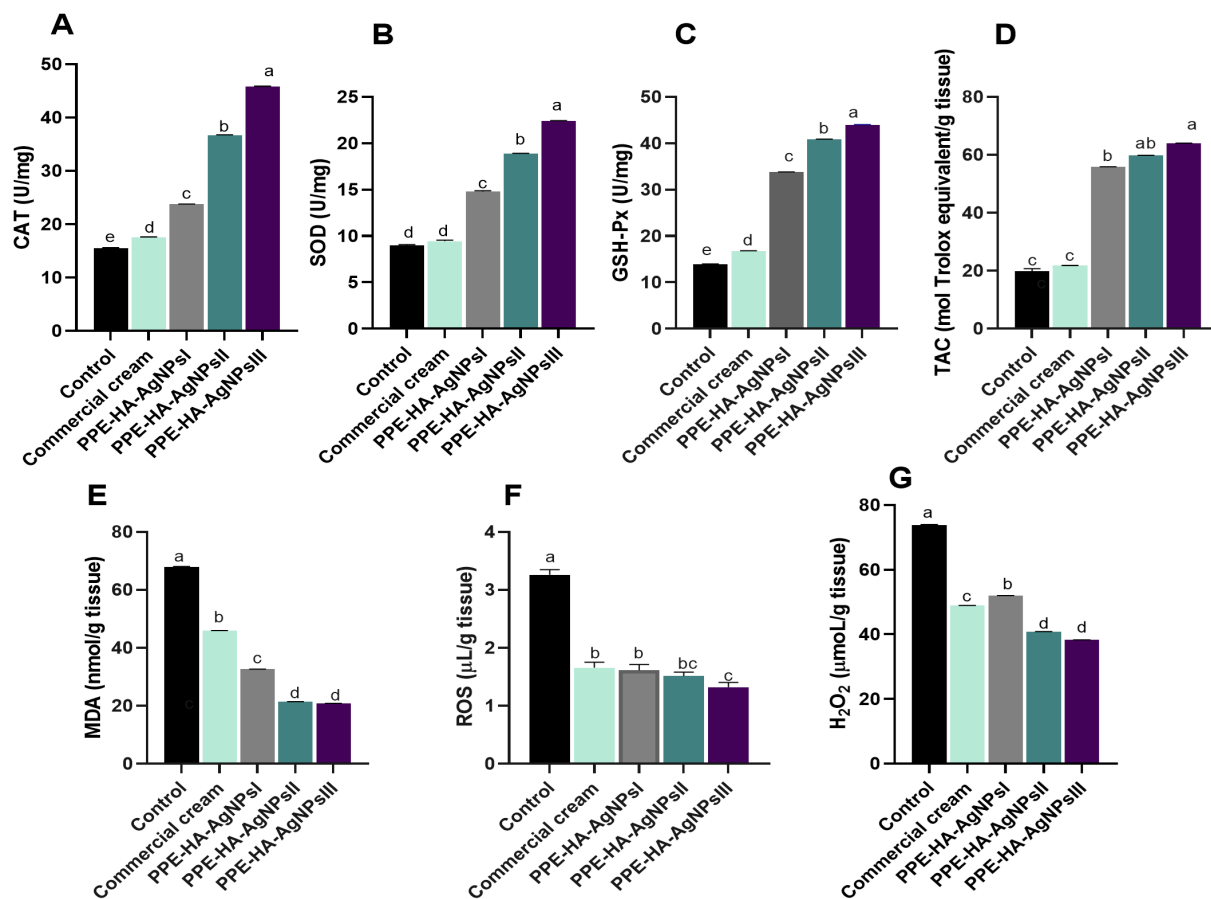


FIGURE 7

The activity of antioxidant enzymes: CAT [catalase, (A)], SOD [superoxide dismutase, (B)] glutathione peroxidase [GSH-Px, (C)], TAC [total antioxidant capacity, (D)], and lipid peroxidation biomarker [MDA, (E)]; and oxidative stress-related biomarkers: ROS [reactive oxygen species, (F)] and H₂O₂ [hydrogen peroxide, (G)] on day 10 post-treatment in response to the therapeutic effects of a hydrogel loaded with pomegranate peel extract-hyaluronic acid-silver nanoparticles (PPE-HA-AgNPs) at different concentrations for 15 days in cutaneous wounds in rats experimentally infected with *C. albicans*. Control: *C. albicans* infected and non-treated rats, commercial cream: ketoconazole cream (2%), PEE-HA-AgNPsI: 25% concentration of the formulated nanocomposite, PPE-HA-AgNPsII: 50% concentration of the formulated nanocomposite, PPE-HA-AgNPsIII: full concentration of the formulated nanocomposite. ^{a–e}Mean values with distinct letters in the same column changed significantly ($p < 0.05$).

cream exhibited the same expression levels of the collagen I gene. Over time, the expression levels of the *VEGF* and *Ang-1* genes gradually decreased with an increase in the PPE-HA-AgNP dose, and the lowest value ($p < 0.05$) was recorded on day 15 post-treatment in the group topically treated with PPE-HA-AgNPsIII (Figure 9). Further RT-qPCR analysis revealed that the *TGF-β1*, *bFGF*, and *EGF* genes had markedly poor expression in the control untreated group. In comparison, their expression levels were increased, reaching their peaks in the PPE-HA-AgNPsIII-loaded-hydrogel-treated group on days 10 and 15 post-treatment. Moreover, the groups treated with PPE-HA-AgNPsIII and ketoconazole cream had no significant difference ($p > 0.05$) regarding the expression of the *TGF-β1* gene on day 15 post-treatment. Five days from the onset of treatment, the expression levels of the *Ki-67* gene reached their maximum in the PPE-HA-AgNPsIII-treated group, followed by PPE-HA-AgNPsII and ketoconazole cream-treated groups. Furthermore, there was a dose-dependent reduction in *Ki-67* gene expression with the lowest reduction found in the PPE-HA-AgNPsIII-treated rats on day 15 post-treatment (Figure 9).

The effect of the PPE-HA-AgNP-loaded hydrogel on the angiogenic and wound healing markers, measured using ELISA assays, is shown in Figure 10. Five days after treatment, all groups were observed to have higher TGF-β1 levels than on day 15 post-treatment, where the biggest reduction was detected in the PPE-HA-AgNPsII and PPE-HA-AgNPsIII-treated groups compared to the control untreated group. All the treated groups had higher Ang-1 and VEGF levels on day 5 post-treatment and their levels were decreased on day 15 post-treatment, especially in the PPE-HA-AgNPsII-treated group. On day 5 post-treatment, all the PPE-HA-AgNP-treated groups exhibited lower *MMP-9* levels in a dose-dependent manner compared with the control untreated group with significant reduction in the PPE-HA-AgNPsIII-treated group on day 15 after treatment.

3.9 Histopathological examination

Histopathological images of the therapeutic effects of PEE-HA-AgNPs at different concentrations in the skin tissue of rats that were

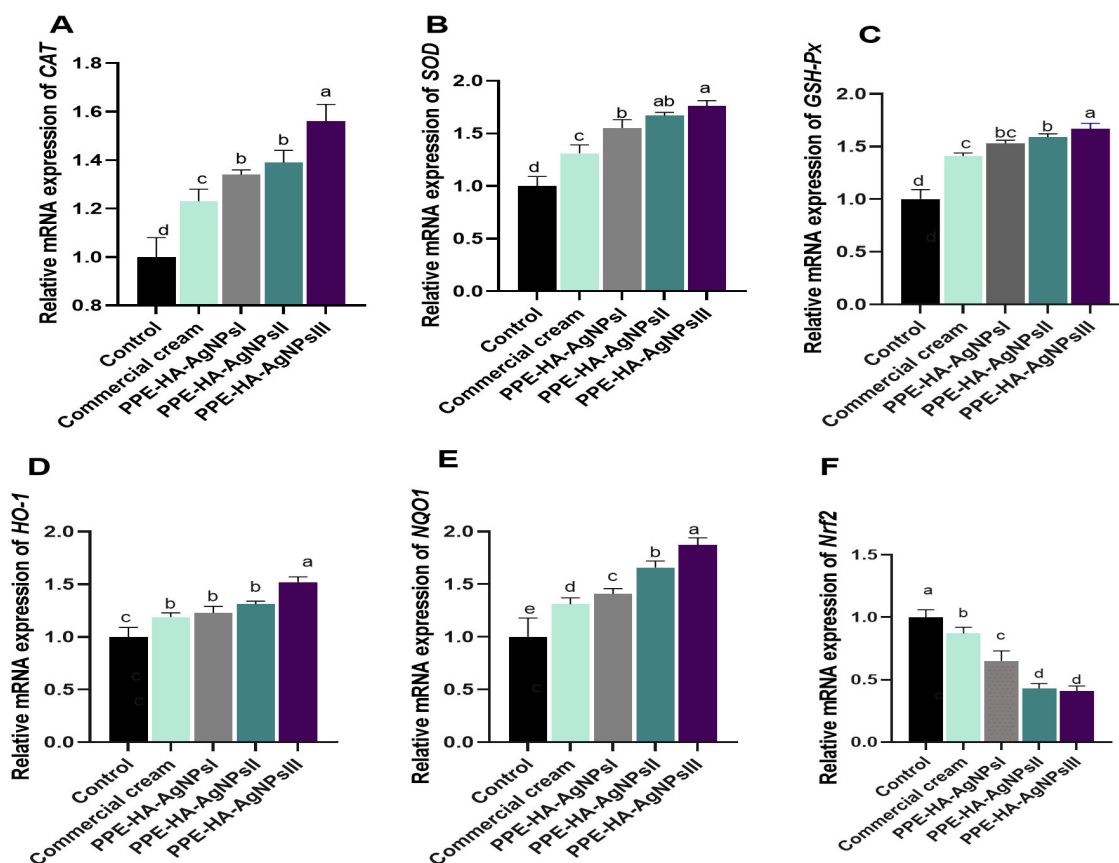


FIGURE 8

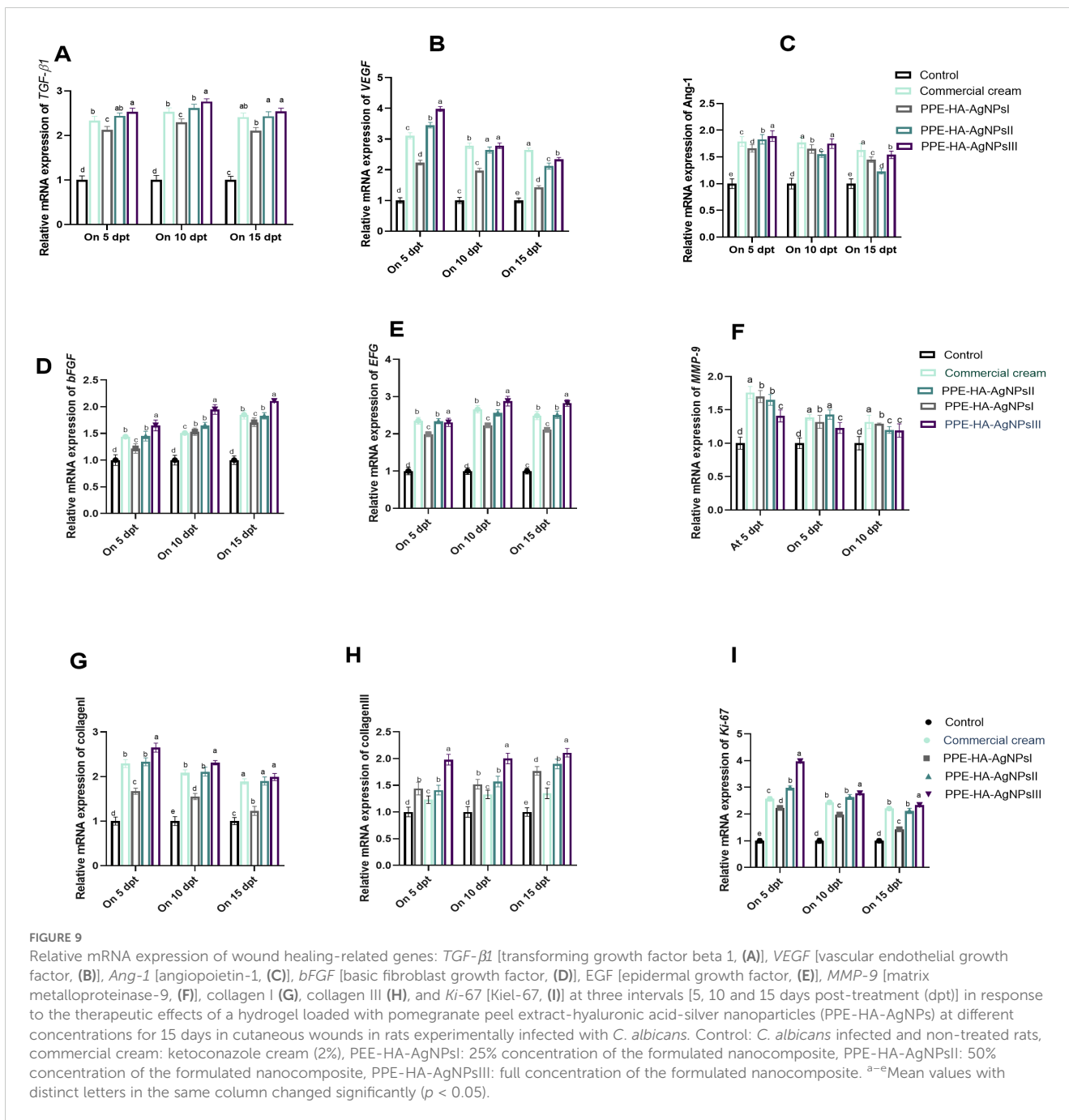
Relative mRNA expression of genes encoding antioxidants response: *CAT* [catalase, (A)], *SOD* [superoxide dismutase, (B)], *GSH-Px* [glutathione peroxidase, (C)], *HO-1* [heme oxygenase-1, (D)], *NQO1* [NAD(P)H quinone oxidoreductase 1, (E)], and *Nrf2* [nuclear factor erythroid 2-related factor 2, (G)] on day 10 post-treatment in response to the therapeutic effects of a hydrogel loaded with pomegranate peel extract-hyaluronic acid-silver nanoparticles (PPE-HA-AgNPs) at different concentrations for 15 days in cutaneous wounds in rats experimentally infected with *C. albicans*. Control: *C. albicans* infected and non-treated rats, commercial cream: ketoconazole cream (2%), PPE-HA-AgNPsI: 25% concentration of the formulated nanocomposite, PPE-HA-AgNPsII: 50% concentration of the formulated nanocomposite, PPE-HA-AgNPsIII: full concentration of the formulated nanocomposite. ^{a-e}Mean values with distinct letters in the same column changed significantly ($p < 0.05$).

experimentally infected with *C. albicans* are shown in Figure 11. The control untreated group showed the most apparent changes in the skin tissue on day 5 following treatment in the form of a gap area filled with crust or hyper eosinophilic hyaline materials that contained filamentous elements, reflecting the presence of *C. albicans*, mixed with leukocytic infiltrates when compared with normal skin histomorphological structure in Figure 11A. Moreover, there was acanthosis, distorted skin appendages, and dermatitis adjacent to this gap area. Meanwhile, on day 15 post-treatment, there was marked acanthosis, spongiosis with prominent finger projections toward the dermal layer beside dilated blood vessels, and leukocytic infiltrates within the dermal layer (Figure 11B). Treatment with the ketoconazole cream showed prominent acanthosis with sub-epidermal inflammatory cell infiltrates and dermal edema on day 5 post-treatment and moderate acanthosis with minute round cell infiltrates adjacent to the sebaceous glands on day 15 post-treatment (Figure 11C). Following treatment with PPE-HA-AgNPsI, intense acanthosis with spongiosis and minute dermal leukocytic infiltrates were encountered on day 5 after-treatment, and mild acanthosis and apparent normal architecture of skin appendages within the dermis were found on day 15 post-

treatment (Figure 11D). Treatment with PPE-HA-AgNPsII resulted in apparent normal configurations of the epidermis, dermis, and skin appendages with few leukocytic infiltrates and hyalinization within the dermal layer on day 5 following treatment and an improvement in the integrity of the skin layers with hyalinizing or mature fibrous tissue within the superficial dermal layer on day 15 post-treatment (Figure 11E). Treatment with PPE-HA-AgNPs at the full concentration relieved the histopathological lesions in *C. albicans*-infected rats evidenced by the normal structure of the epidermis, dermis, and skin appendages with a minute area of hyalinizing fibrous tissue within the superficial dermal layer on day 5 after treatment and histologically normal structures of the epidermis, dermis, and skin appendages on day 15 post-treatment (Figure 11F).

4 Discussion

Wound healing problems are serious therapeutic challenges among other healthcare concerns. Proper cutaneous wound healing is fundamental for the restoration of disrupted anatomical stability



and the functional status of the skin (Okur et al., 2020). However, improper wound healing could result in the invasion of pathogenic microorganisms with progression to disadvantageous clinical complications and increased risk to the patients and treatment costs (Scappaticci et al., 2021). *C. albicans* is the most prevalent human pathogen worldwide and a major contributor to wound infections (Brown et al., 2012), and it is considered an emerging resistant fungal pathogen of the skin that can result in life-threatening infections with possible mortality in healthcare settings and hospitals (Gil et al., 2022). Up till now, antifungal therapy has been restricted for *C. albicans* due to the emergence of drug resistance against the current antifungals and the low effectiveness of topical drug penetration. Therefore, the

development of novel efficient evidence-based therapy, combining nanotechnology and phytotherapy, for candidiasis, and in particular, those with long-lasting effects and targeting biofilms is urgently required. Thus, the current study showed that nanocomposite-loaded hydrogel therapy combining PPE, HA, and AgNPs can effectively exert antifungal activity against *C. albicans*, and it was found to be efficient in wound healing. One important factor that contributes to the pathogenesis of candidiasis is biofilm formation as *C. albicans* has the ability to form biofilms on both inert and biological surfaces (Taff et al., 2013). The current study showed that the infected and non-treated group exhibited the greatest colonization and invasion of *C. albicans* inside or around the wound area, while the lowest colonization and invasion were

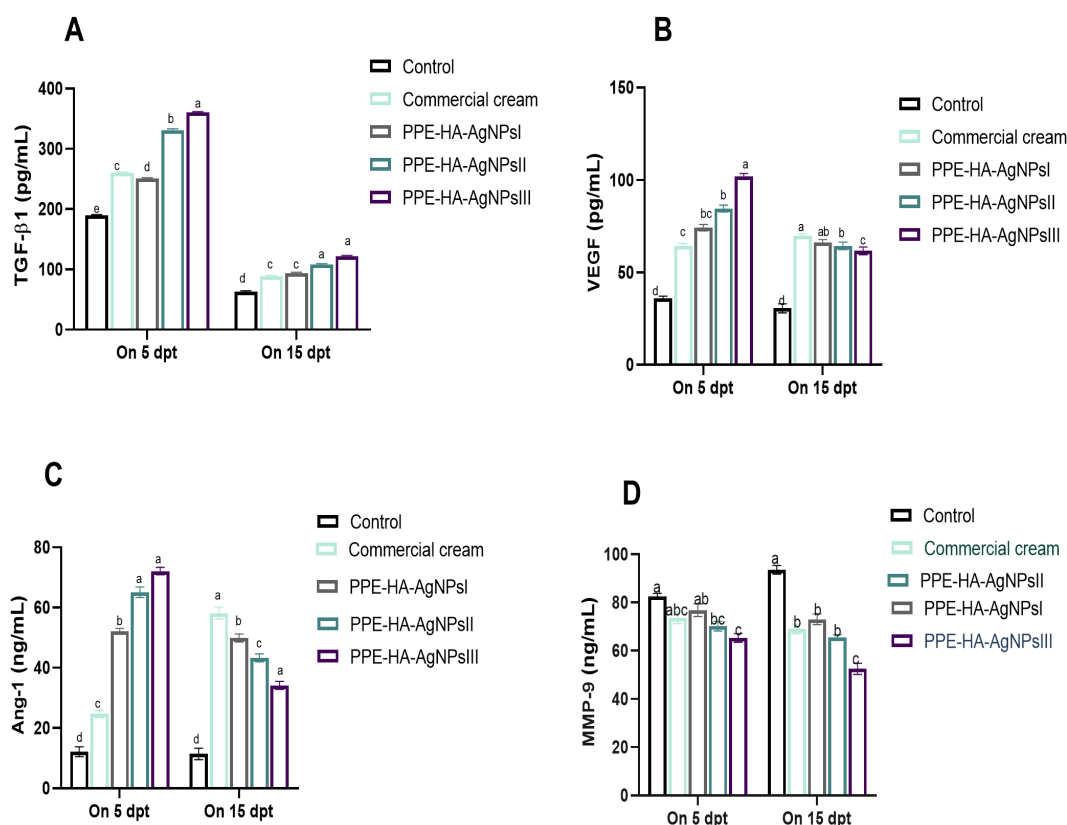


FIGURE 10

ELISA estimation of wound healing-related markers: TGF-β1 [transforming growth factor beta 1, (A)], VEGF [vascular endothelial growth factor, (B)], Ang-1 [angiopoietin-1, (C)], and MMP-9 [matrix metalloproteinase-9, (D)] at two intervals [5 and 15 days post-treatment (dpt)] in response to the therapeutic effects of hydrogel loaded with pomegranate peel extract-hyaluronic acid-silver nanoparticles (PPE-HA-AgNPs) at different concentrations for 15 days in cutaneous wounds in rats experimentally infected with *C. albicans*. Control: *C. albicans* infected and non-treated rats, commercial cream: ketoconazole cream (2%), PPE-HA-AgNPsI: 25% concentration of the formulated nanocomposite, PPE-HA-AgNPsII: 50% concentration of the formulated nanocomposite, PPE-HA-AgNPsIII: full concentration of the formulated nanocomposite. ^{a-e}Mean values with distinct letters in the same column changed significantly ($p < 0.05$).

detected in the group treated with the highest concentration of PPE-HA-AgNPs. Additionally, the *C. albicans* biofilm was inhibited by a 55% concentration of PPE, which is mainly attributed to its phenolic compounds (de Almeida Rochelle et al., 2016). The aforementioned findings reveal that the combination of HA-AgNPs and PPE in a nano hydrogel composite exhibited effective fungicidal activity.

In comparison with the group treated with a commercial cream of azole derivatives, the group treated with PPE-HA-AgNPs at full concentration showed higher antifungal and antibiofilm potency, which were evidenced by a lower *C. albicans* burden and the downregulation of its biofilm-related genes. Accordingly, the antibiofilm effects of AgNPs treatment were outer cell membrane disruption and *C. albicans* filament inhibition (Lara et al., 2015). The mechanistic action of metallic NPs involves the disruption of the cell walls, leading to an increase in their permeation owing to the electrostatic interaction between positively charged NPs and negatively charged cell wall molecules of the microorganism, resulting in cytoplasmic content leakage (Joshi et al., 2020) and membrane potential disorders (Taff et al., 2013). Additionally, AgNPs exert their anti-fungal activity via the permeabilization of target cell membranes, destruction of proton pumps, and denaturation

of proteins after the interaction with phosphoric and sulfur groups that exist on the surface of the fungal cell wall (Dulińska-Litewka et al., 2021). Furthermore, treatment with erodium glaucophyllum loaded-AgNPs resulted in declines in the counts of fungal cells and lesion rates, suggesting their prospective use in the treatment of oral candidiasis (Abdallah and Ali, 2022). Additionally, metallic NPs can potentiate ROS generation, as another mechanism for killing pathogenic microorganisms (Canaparo et al., 2020) which aligns with our findings following the treatment with PPE-HA-AgNPs. The fungicidal capacity of AgNPs was explained by their aggregation outside the fungal cells, the release of their silver ions, and thus the generation of cell death via the reduction process resulting from the interaction of ionic silver with cell components (Vazquez-Muñoz et al., 2014). Together with the antifungal efficacy of AgNPs, recent studies have revealed that PPE is an attractive natural anti-fungal alternative against wide varieties of fungal pathogens owing to its active inhibitors including phenolics and flavonoids (Dahham et al., 2010; Sadeghian et al., 2011). Additionally, the significant inhibitory antifungal effect of pomegranate water extract against *C. albicans* has been reported (Tayel and El-Tras, 2010). The anticandidal potentiality of a free form of PPE in a previous study was explained by the synergistic effect of their combined constituents,

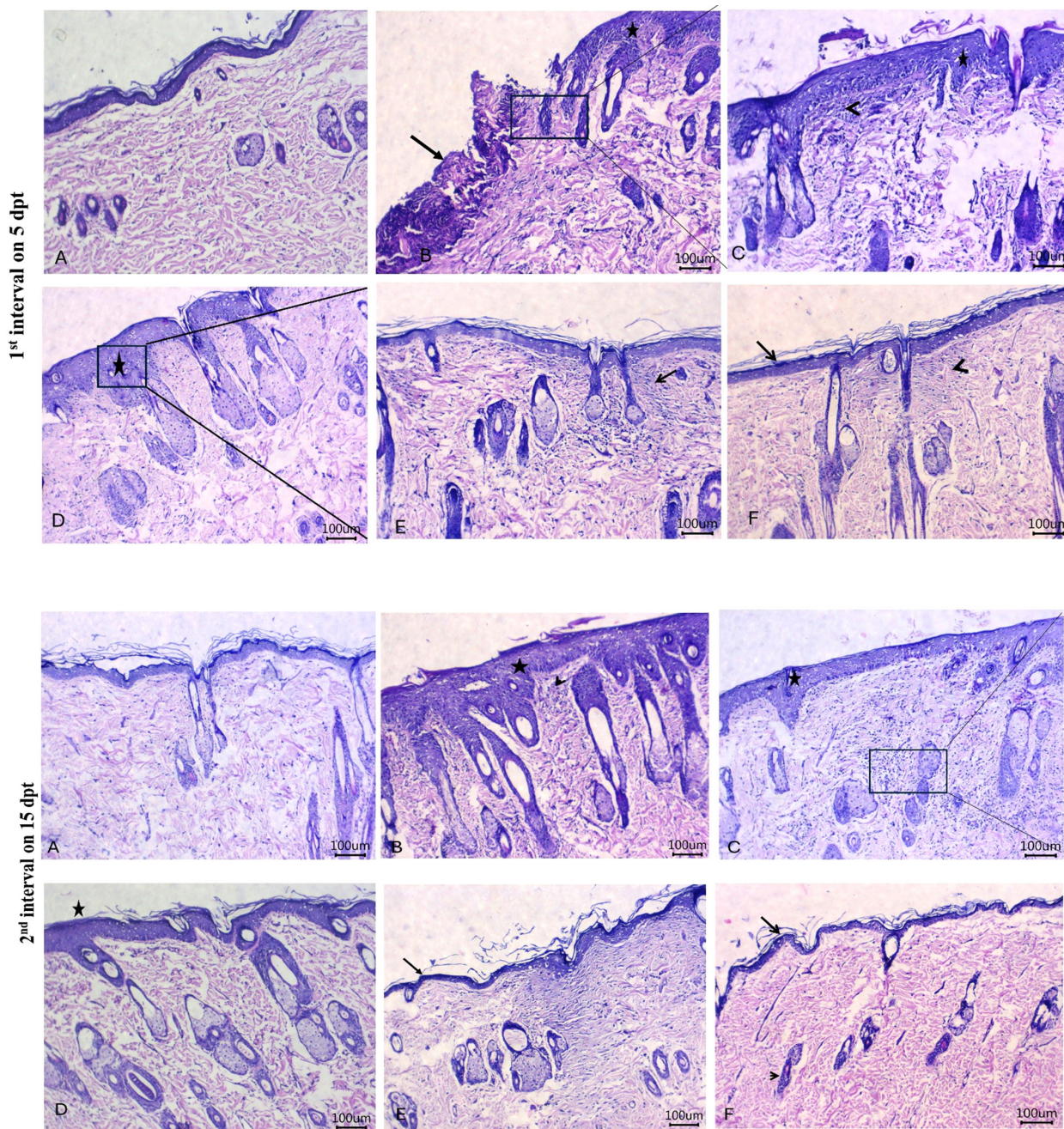


FIGURE 11
 Histopathological images of skin tissues of rats experimentally infected with *C. albicans* in response to the therapeutic effects of a hydrogel loaded with pomegranate peel extract-hyaluronic acid-silver nanoparticles (PEE-HA-AgNPs) at different concentrations for 15 days on 5 (1st interval) and 15 (2nd interval) dpt (days post-treatment). 1st interval: normal skin tissues of non-infected rats (A); *C. albicans* infected and non-treated rats showing gap areas filled with crust or hyper-eosinophilic hyaline materials (arrow) with leukocytic infiltrates beside acanthosis (star) (B); ketoconazole cream- (2%) treated rats showing acanthosis (star) with sub-epidermal inflammatory cells infiltrates (arrowhead) (C); PEE-HA-AgNP- (25%) treated rats revealing intense acanthosis (star) with spongiosis (arrow) (D); PEE-HA-AgNP- (50%) treated rats displaying apparent normal configurations of the epidermis, dermis, and skin appendages with few leukocytic infiltrates (arrow), and hyalinization (arrowhead) within the dermal layer (E); and PEE-HA-AgNP- (100%) treated rats exhibiting normal structures of the epidermis (arrow), dermis, and skin appendages with a minute area of hyalinizing fibrous tissue within the superficial dermal layer (arrowhead) (F). 2nd interval: normal skin tissues of non-infected rats showing normal histomorphological structure of the epidermal layer with a superficial keratin layer and a normal dermal layer with associated skin appendages (A); *C. albicans* infected rats showing marked acanthosis, spongiosis (star) with prominent finger projections toward the dermal layer beside dilated blood vessels and leukocytic infiltrates (arrowhead) within the dermal layer (B); ketoconazole cream- (2%) treated rats showing moderate acanthosis (star) with minute round cells' infiltrates adjacent to sebaceous glands (C); PEE-HA-AgNP- (25%) treated rats revealing mild acanthosis (star) and apparent normal architecture of skin appendages within the dermis (D); PEE-HA-AgNP- (50%) treated rats displaying apparently normal epidermis (arrow) and dermis layers with hyalinizing or mature fibrous tissue within the superficial dermal layer (arrowhead) (E); and PEE-HA-AgNP- (100%) treated rats exhibiting normal histological structures in the epidermis (arrow), dermis, and skin appendages (arrowhead) (F). Scale bar 100 µm.

which include powerful antibacterial and antifungal compounds (Seeram et al., 2006). In the current study, the long-lasting antifungal impact and optimal functionality of the novel nanocomposite formulated with PPE-HA-AgNPs are linked to its higher biodegradability and the controlled release of active biomolecules in the infected wound area, which accelerate healing.

The wound healing process involves multiple distinct and overlapping inflammatory and granulation phases, including hemostasis/inflammation, proliferation, fibrogenesis, neovascularization, wound contraction, and epithelialization (Wang et al., 2018). During the course of an injury, the inflammation process assists by eliminating damaged cells and promoting vasoconstriction (Yuniarti et al., 2018). Furthermore, the recruitment of immune cells such as neutrophils and macrophages results in the production of proinflammatory mediators such as interleukins and cytokines and the equilibrated scenario of inflammatory response generally happens. However, prolonged inflammatory events can become a chronic situation that is dangerous for the wound-healing process (Kiritsi and Nyström, 2018). In the current study, the combined curative impact of PEE, HA, and AgNPs not only reduced fungal colonization in the skin tissue of the rat model but also decreased the excessive inflammatory response associated with infected wounds. Herein, the groups topically treated with higher concentrations of PPE-HA-AgNPs showed decreased exaggerated inflammatory responses that triggered tissue damage during wound healing as proved by the reduction in the levels of *TNF- α* , *IL-6*, and *IL-1 β* in the skin in a dose-dependent manner, especially at 10 days post-treatment, which was in conjunction with the downregulation of cytokine-related genes (*IL-1 β* , *IL-6*, *IL-18*, and *TNF- α*). In addition, the immune-stimulatory role of PPE-HA-AgNPs was shown by the increase in anti-inflammatory cytokine production, especially IL-10. *TNF- α* , *IL-6*, and *IL-1 β* are proinflammatory cytokines that are over-secreted and expressed during the inflammatory phase in a variety of disease states (Scheller et al., 2011). The inhibition of aggravated expression of proinflammatory cytokines and boosting the expression of anti-inflammatory cytokines are essential healing mechanisms (Abraham and Kappas, 2008). In the same way, using natural compounds as a substitute for chemical ones triggers healing with satisfactory results (Dwivedi et al., 2017; Shen et al., 2017). The use of pomegranate extracts to accelerate the healing process has previously been described (Elzayat et al., 2018; Lukiswanto et al., 2019).

Moreover, the antimicrobial and anti-inflammatory properties of pomegranate are due to the presence of phenolic acids and flavonoids that have an active role in wound healing (Salama et al., 2021). Moreover, HA possesses the capability to inhibit inflammatory events such as cytokine and prostaglandin production (Shalumon et al., 2018). The anti-inflammatory properties of pomegranate extracts are of great interest, and punicalagin is highly implicated in this anti-inflammatory ability (El-Missiry et al., 2015). Moreover, pomegranate extract with 40% ellagic acid accelerated the healing of deep second-degree burn wounds due to its anti-inflammatory properties (Lukiswanto et al., 2019). The anti-inflammatory properties of acetone extract from whole pomegranate fruit resulted in phosphorylation inhibition of the release of numerous cytokines, and the mechanism underlying this was observed to be NF- κ B-dependent (Colombo et al., 2013).

Furthermore, punicalagin in PPE can regulate signaling pathways in inflammation-associated disorders by reducing the production of *TNF α* -induced expressions of pro-inflammatory cytokines, including *IL-1 β* , *IL-6*, and *IL-8* (BenSaad et al., 2017; Venusova et al., 2021). In addition, AgNPs could reduce inflammation by inhibiting the release of pro-inflammatory cytokines, such as *IL-6*, and decreasing CRP levels, thereby promoting wound repair (Liu et al., 2010). Another beneficial outcome, beyond the topical application of PPE-HA-AgNPs, is the regulation of redox balance in infected wounds through the modulation of ROS and antioxidant levels. The inflammatory process in infected wounds can induce oxidative stress and reduce cellular antioxidant capacity and, in this way, exaggerated ROS production can distribute redox homeostasis membrane lipids and modulate DNA and protein structures (Dwivedi et al., 2014). In addition, H_2O_2 is a prominent secondary intracellular messenger that regulates various stages of wound healing including cell recruitment, cytokine production, cell proliferation and migration, and angiogenesis (Bryan et al., 2012). Moreover, HO-1 is an enzyme that dissociates heme and produces antioxidant molecules, iron ions, and carbon monoxide that control the principal processes involved in apoptosis, inflammation, and cell angiogenesis and proliferation (Loboda et al., 2016). Throughout wound healing, Nrf2 decreases oxidative stress in cells, has a fundamental role in the proliferation of epithelial cells' apoptosis and migration (Long et al., 2016), and controls MMP-9 levels (Jindam et al., 2017). Interestingly, in the present study, we proved that PPE-HA-AgNPs topical application enhanced antioxidant status and notably decreased oxidative stress biomarkers compared with the control untreated or even commercially treated groups. These findings were supported by a significant increase in SOD, GSH-Px, and catalase activity and TAC levels with a simultaneous decrease in ROS, H_2O_2 , and MDA levels in the skin tissues. At the molecular level, a significant upregulation of HO-1, NQO1, Nrf2, and other antioxidant-related genes was detected following the administration of PPE-HA-AgNPs, which aligns with the findings of Sayed et al. (2022). Similarly, the antioxidant functions of the active constituents in pomegranate can counteract oxidative stress by maintaining MDA, glutathione, catalase, and peroxidase levels (Kaur et al., 2015). Sreekumar et al. (2014) stated that combining pomegranate with silver promotes wound healing, accelerates epithelialization, and enhances remodeling due to the free radical scavenging and antioxidant activity of polyphenols. Additionally, the quantification of wound fluid nitrate in the form of NO bioactivity in the wound healing process suggested a diagnostic role in good wound healing (Boykin, 2010). Emerging evidence indicates that NO plays a central role in wound healing, including angiogenesis and migration and proliferation of fibroblasts, epithelial cells, endothelial cells, and keratinocytes (Gallagher et al., 2007). It also facilitates intercellular communication to regulate cell proliferation and collagen production (Witte and Barbul, 2002). An optimal release of NO would improve wound healing; however, over-production of NO over time can result in the development of chronic wounds (Barrientos et al., 2008). In accordance with these findings, the NO and NOS activity in PPE-HA-AgNP-treated rats was lower than that in the non-treated ones, especially at 10 days after

treatment. These potentiated antioxidant outcomes of PPE-HA-AgNPs are mainly owing to the polyphenolic molecules of the pomegranate peel extract which exert potent antioxidant activities with wound healing and anti-allergic properties that reduce skin damage via their free radical scavenging power, which is in accordance with Salama et al. (2021). Additionally, the nanoformulation of PPE can prolong the release of active substances, thus optimizing its therapeutic delivery (Paczkowska-Walendowska et al., 2024). On the other hand, the remarkable effect of PPE-HA-AgNPs was explained by the gelling characteristics of HA, which acts as a hydrophobic agent that augments the efficacy of AgNPs due to the enhancement of the transportation mechanism via the cellular membrane with prolonged therapeutic activity owing to its size (Ivashchenko et al., 2018). Moreover, the prolonged pharmacological effect in rats of HA is a result of the drug release and delivery in a nano-form (Liu et al., 2018). Besides, Makvandi and co-workers (Makvandi et al., 2019) showed that hydrogels comprising AgNPs, HA, and corn silk extract exhibited adequate biocompatibility. Additionally, their application brings about excellent wound closure and a smaller wound area compared to the control samples in a wound healing assay. Another explanation is that wound dressings with a combination of nano-silver and HA are extremely hygroscopic, facilitating the removal of excessive exudates from the wound beds (El-Aassar et al., 2020). They also have an excellent rate of water-vapor transmission and are consequently capable of preventing dryness and dehydration of wounds, providing an appropriate environment for the regeneration of skin tissues (Tarusha et al., 2018). Moreover, the effectiveness of PPE-HA-AgNPs at a higher concentration was supported by histopathological examination that showed a decrease in exaggerated inflammatory response, replacement of necrotic tissues with granulation ones along with reduced cellularity, and increased collagen deposition and skin re-epithelialization. In accordance, a methanolic extract of pomegranate peels had an enhanced healing capability by ameliorating the histopathological picture in excision cutaneous wounds in diabetic rats (Karim et al., 2021). Additionally, pomegranate fractions promote proliferation, procollagen synthesis, and thus the regeneration of the dermis and epidermis (Aslam et al., 2006). Moreover, another study that utilized AgNPs and pomegranate formulations in diabetic rats showed that the quantification of inflammatory infiltrates was greatly reduced in histological pictures after treatment (Scappaticci et al., 2021).

During tissue repair, inflammatory cells stimulate the migration and proliferation of endothelial cells, leading to neovascularization. This process involves connective tissue cells synthesizing extracellular matrices, including collagen, as well as keratinocytes, which contribute to the re-epithelialization of the wounded tissue (Olczyk et al., 2014). Collagen, a major extracellular protein matrix, is the component that ultimately contributes to wound strength (Chithra et al., 1998). Additionally, collagen molecules play a fundamental role in wound contraction and maintaining tissue matrix integrity, both of which are crucial for effective wound healing. Types I and III collagen are the primary types involved in wound repair, and their ratio remains constant in normal skin. However, in mature scar tissue formed after trauma, the ratio of

type I collagen is greater than that in normal skin (Hu et al., 2023). In line with these findings, the rats in the groups topically treated with PPE-HA-AgNP-loaded hydrogel showed enhanced healing signs for cutaneous wounds via improvement in wound size, contraction, and closure together with a lower expression of the MMP gene and higher expression of the collagen I and III genes. This revealed increased fibroblast proliferation and collagen regeneration that provided negative entities for pathogenic microorganisms such as *C. albicans*, promoting wound healing. In accordance, a free form of a water-soluble extract made from pomegranate peel was found to inhibit the elaboration of the major MMP-1 enzyme which is responsible for collagen destruction in aged/photoaged skin (Brennan et al., 2003). Moreover, it was found that MMP-1 accumulation in the fibroblast-conditioned medium was dramatically reduced in the presence of the pomegranate peel extract (Aslam et al., 2006). Additionally, a therapeutic synergistic strategy based on Au/Ag nanodots resembling a pomegranate-like core in a polyvinyl alcohol hydrogel had an efficient treatment impact on diabetic wounds via their superior anti-inflammatory properties with accelerated collagen deposition capacity (Wang et al., 2023).

Additionally, an imbalance of cytokine expression and growth factors, increased activity of metalloproteinase, and oxidative stress can impair neo-angiogenesis and result in cell dysfunction and wound healing retardation (Bannon et al., 2013). During the process of natural wound healing, angiogenic activity primarily results in the formation of a disorganized vascular network at the injury site, characterized by an increased number of blood vessels. Once vessel density reaches its peak, vascular remodeling occurs, marked by the regression of the vascular network and the gradual maturation of blood vessels (Urciuolo et al., 2019). Many angiogenic growth factors and signaling pathways are involved in early vascular development, among these are VEGF, bFGF, Ang, and TGF- β (Crivellato, 2011). VEGF appears to be a key factor in pathological events such as tissue repair, which involves neovascularization and increased vascular permeability (Santos et al., 2007). Moreover, it improves angiogenesis during wound healing by stimulating the migration of endothelial cells through the extracellular matrix. In contrast, abnormal angiogenesis can result from inflammatory stimulation (Hu et al., 2023). FGF signaling has a critical role in efficient healing, while its deficiency reflects a state of wound healing impairment (Ortega et al., 1998). Furthermore, TGF- β can promote cells to enhance extracellular matrix protein synthesis and concurrently reduce collagen proteases (El Gzaerly et al., 2013). Herein, significant increases in pro-angiogenic markers reflected by the higher expression of the *Ang-1* and *VEGF* genes in the created cutaneous wounds treated with PPE-HA-AgNPs were remarkably detected between 5 dpt and 10 dpt and gradually decreased by 15 dpt. Moreover, a significant increase in re-epithelialization markers together with deposition of collagen fibers, which were supported by the upregulation of *TGF- β 1*, *bFGF*, *EFG*, and collagen I and III genes post-treatment with a higher concentration of PPE-HA-AgNPs, indicated faster and successful wound healing. These findings were also supported by the ELISA results for markers associated with wound healing as established in an earlier study (Zhou et al., 2017). We hypothesized

that the presence of PPE-HA-AgNPs enhanced TGF- β availability in the extravascular environment by priming cells, boosting their response to the normal regulatory factors at the site of injury. These findings were in agreement with a previous study (Özkan et al., 2004), where in the first week after injury, higher neovascularization was crucial for providing oxygen and necessary nutrients to the wound site and initiated granulation tissue formation.

In the same context, Elbially et al. (2020) found that the significant gene expression levels of *bFGF* and *VEGF* to the remarkable wound healing process led to enhanced angiogenesis and collagen deposition with improved epithelialization rate. These results can be linked to the scavenging effects of PPE-enriched flavonoids, as proven by the low ROS levels detected in the current study, which are required to activate cell signaling pathways and angiogenesis, participating in the elimination of invading pathogens. Inversely, high ROS levels in the non-treated rats triggered oxidative stress that seriously compromised tissue repair, resulting in unhealed wounds that can be painful and require expensive and long-term treatments as proven previously (Dunnill et al., 2017). Similarly, given the potent angiogenic and antioxidant activities of flavonoids, unique sets of nanocomposite membranes delivering them were prepared for wound-healing applications (Lee et al., 2014). Proper wound healing was also reinforced by HA naturally occurring in the extracellular matrix with structural and biological properties mediating its activity in the matrix organization (Um et al., 2004). In accordance, epigallocatechin gallate enhanced diabetic wound healing by activating the expression of angiogenesis-related genes and decreasing the expression of inflammation-related genes (Hu et al., 2023). A herbal extract enriched with ellagic acid is expected to accelerate angiogenesis-related markers (Nirwana et al., 2022). In addition, angiogenic activity by an active ingredient of PPE such as punicalagin in this study could contribute to the processes of tissue repair and wound healing as previously documented by Carneiro et al. (2016). Furthermore, ELISA assays supported by qRT-PCR results revealed that VEGF expression in wound tissues of rats treated with a methanolic extract based-gel from a Saudi pomegranate peel gel was significantly higher than that in diabetic non-treated rats (Karim et al., 2021). Moreover, Dai et al. (2021) stated that matrix metalloproteinase plays an important role in the normal wound remodeling process as it can enzymatically dissociate tissue extracellular matrix and mediate cell migration, while excessive MMP-9 production can prevent wound healing. Herein, the expression of the *MMP-9* gene in wound tissue specimens of rats following treatment with PPE-HA-AgNPs was dose-dependently lower than that in the traditionally treated rats. In accordance, various bioactive pomegranate fractions might inhibit the elaboration of the major enzyme, MMP, which is responsible for skin collagen destruction, in agreement with previous studies (Aslam et al., 2006; Brennan et al., 2003). Increased cell proliferation is a crucial aspect of wound healing, in general, and the Ki-67 protein is an important marker of this cellular event. Ki-67 expression is also widely known to be an indicator of cell growth within a total cell population (Choi et al., 2012). The current study established an increased expression of *Ki-67* gene with an increasing dose of PPE-

HA-AgNPs compared with the traditionally treated group suggesting that the prepared nanocomposite increased cell proliferation and the consequent stimulus for the remodeling phase. Furthermore, the beneficial effects of the formulated nanocomposite could result from its incorporation into an efficient nanocarrier that stimulates the abovementioned cellular and molecular processes, aiding in the wound microenvironment. This was owing to its distinct antimicrobial, anti-inflammatory, and angiogenic effects and better adsorption and loading capacity that possibly changed the wound's milieu from a non-healing to a healing state (Kushwaha et al., 2022).

The aforementioned findings were also supported by the healing effect of the PPE-HA-AgNPs on wound tissue regeneration in the histological examinations that demonstrated an improvement in the integrity of the skin layers with hyalinizing or mature fibrous tissue within the superficial dermal layer on day 15 post-treatment. In contrast, the untreated infected group showed the most pronounced changes in the skin tissues of rats on day 5 post-treatment, characterized by gap areas filled with crusts or hyper-eosinophilic hyaline materials containing filamentous elements, indicative of the presence of *C. albicans*. Furthermore, marked acanthosis, spongiosis with prominent finger projections toward the dermal layer beside dilated blood vessels, leukocytic infiltrates within the dermal layer, and distorted skin appendages were detected in this group. Notably, the higher concentration of PPE-HA-AgNPs caused a complete regeneration of the epidermis and dermis, and a new epithelium was visible as apparent skin appendages with prominent wound contraction and no evidence of filamentous elements reflecting the presence of *C. albicans*. Similarly, post-AgNDs@Gel + NIR treatment, the histological view of skin wounds was improved with complete healing, evidenced by enhanced formation of epidermis and dermis tissue (Wang et al., 2023).

5 Conclusion

The favorable effects of PPE-HA-AgNPs on the healing of *C. albicans* infected wounds seem to be mainly due to the innovative nano-delivery system. PPE exerts its potential functions by reducing the ability of free radicals to generate tissue damage, augmenting antioxidant status, and diminishing inflammatory markers with enhanced collagen deposition and antifungal activity. Moreover, the mechanism of action of metallic AgNPs against *C. albicans* was found to be the modification of biofilm-specific genes which maintain sustained inflammation and delay wound healing. Based on our results, we conclude that PPE-HA-AgNPs accelerate the healing of cutaneous wounds infected with *C. albicans* via various mechanisms including an extended-release with better retention ability on the skin surface, reducing the exaggerated inflammatory response, and promoting new granulation tissues, angiogenesis, and skin re-epithelialization. Therefore, our findings demonstrate the wound-healing potential of PPE-HA-AgNPs as a promising therapeutic agent against cutaneous wounds infected with *C. albicans*.

Data availability statement

The original data presented in the study are included in the article/supplementary material. Further inquiries can be directed to the corresponding author.

Ethics statement

All Animal housing and management protocols were approved by Mansura University Animal Ethical Committee. Ethical approval was attained prior to the commencement of the experimental study and all animal experiments were conducted in conformity with ethics and guidelines of Institutional Animal Care and Use Committee of Faculty of Veterinary Medicine, Mansura University, (MU-ACUC, VM.R.24.05.168). The study was conducted in accordance with the local legislation and institutional requirements.

Author contributions

ME: Conceptualization, Formal Analysis, Funding acquisition, Investigation, Methodology, Validation, Visualization, Writing – original draft. AA: Conceptualization, Formal Analysis, Funding acquisition, Investigation, Methodology, Project administration, Resources, Supervision, Writing – original draft, Writing – review & editing. OM: Conceptualization, Funding acquisition, Investigation, Methodology, Resources, Supervision, Validation, Writing – review & editing. IP: Conceptualization, Data curation, Formal Analysis, Funding acquisition, Methodology, Validation, Visualization, Writing – original draft, Writing – review & editing. SK: Conceptualization, Funding acquisition, Investigation, Methodology, Project administration, Resources, Writing – original draft. SE: Conceptualization, Project administration, Resources, Writing – original draft, Writing – review & editing. SE-B: Conceptualization, Data curation, Formal analysis, Investigation, Methodology, Project administration, Resources, Supervision, Writing – original draft, Writing – review & editing.

References

- Abdallah, B. M., and Ali, E. M. (2022). Therapeutic Effect of Green Synthesized Silver Nanoparticles Using Erodium glaucophyllum Extract against Oral Candidiasis: *In Vitro* and *In Vivo* Study. *Molecules* 27, 4221. doi: 10.3390/molecules27134221
- Abou Hammad, A. B., Hemdan, B. A., and El Nahrawy, A. M. (2020). Facile synthesis and potential application of NiO. 6ZnO. 4Fe₂O₄ and NiO. 6ZnO. 2CeO. 2Fe₂O₄ magnetic nanocubes as a new strategy in sewage treatment. *J. Environ. Manage* 270, 110816. doi: 10.1016/j.jenvman.2020.110816
- Abraham, N. G., and Kappas, A. (2008). Pharmacological and clinical aspects of heme oxygenase. *Pharmacol. Rev.* 60, 79–127. doi: 10.1124/pr.107.07104
- Aggarwal, B. B., Gupta, S. C., and Sung, B. (2013). Curcumin: an orally bioavailable blocker of TNF and other pro-inflammatory biomarkers. *Br. J. Pharmacol.* 169, 1672–1692. doi: 10.1111/bph.12013
- Aldakheel, F. M., Sayed, M. M. E., Mohsen, D., Fagir, M. H., and El Dein, D. K. (2023). Green synthesis of silver nanoparticles loaded hydrogel for wound healing: systematic review. *Gels* 9, 530. doi: 10.3390/gels9070530
- Alherz, F. A., Negm, W. A., Elekhawy, E., El-Masry, T. A., Haggag, E. M., Alqahtani, M. J., et al. (2022). Silver nanoparticles prepared using encephalartos laurentianus de

AM: Conceptualization, Data curation, Formal Analysis, Resources, Visualization, Writing – original draft. LA: Resources, Software, Supervision, Validation, Visualization, Writing – review & editing. AA: Funding acquisition, Investigation, Methodology, Project administration, Writing – original draft. AE: Formal Analysis, Resources, Software, Supervision, Validation, Visualization, Writing – review & editing. SE: Conceptualization, Data curation, Methodology, Project administration, Resources, Writing – original draft. MA: Conceptualization, Funding acquisition, Investigation, Methodology, Project administration, Software, Writing – review & editing. DI: Conceptualization, Data curation, Formal Analysis, Investigation, Methodology, Project administration, Resources, Supervision, Writing – original draft, Writing – review & editing.

Funding

The author(s) declare financial support was received for the research, authorship, and/or publication of this article. This work was supported by the research support project (RSP2024R94) at King Saud University, Riyadh, Saudi Arabia.

Conflict of interest

The authors declare that the research was conducted in the absence of any commercial or financial relationships that could be construed as a potential conflict of interest.

Publisher's note

All claims expressed in this article are solely those of the authors and do not necessarily represent those of their affiliated organizations, or those of the publisher, the editors and the reviewers. Any product that may be evaluated in this article, or claim that may be made by its manufacturer, is not guaranteed or endorsed by the publisher.

wild leaf extract have inhibitory activity against candida albicans clinical isolates. *J. Fungi* 8, 1005. doi: 10.3390/jof8101005

Aslam, M. N., Lansky, E. P., and Varani, J. (2006). Pomegranate as a cosmeceutical source: Pomegranate fractions promote proliferation and procollagen synthesis and inhibit matrix metalloproteinase-1 production in human skin cells. *J. Ethnopharmacol* 103, 311–318. doi: 10.1016/j.jep.2005.07.027

Bancroft, J. D., and Gamble, M. (2008). *Theory and Practice of Histological Techniques*. 6th Edition, Churchill Livingstone, London: Elsevier.

Bannon, P., Wood, S., Restivo, T., Campbell, L., Hardman, M. J., and Mace, K. A. (2013). Diabetes induces stable intrinsic changes to myeloid cells that contribute to chronic inflammation during wound healing in mice. *Dis. Model. Mech.* 6, 1434–1447. doi: 10.1242/dmm.012237

Barrientos, S., Stojadinovic, O., Golinko, M. S., Brem, H., and Tomic-Canic, M. (2008). Growth factors and cytokines in wound healing. *Wound Repair Regen.* 16, 585–601. doi: 10.1111/j.1524-475X.2008.00410.x

Barros, M., Santos, D., and Hamdan, J. S. (2007). Evaluation of susceptibility of Trichophyton mentagrophytes and Trichophyton rubrum clinical isolates to antifungal

- drugs using a modified CLSI microdilution method (M38-A). *J. Med. Microbiol.* 56, 514–518. doi: 10.1099/jmm.0.46542-0
- BenSaad, L. A., Kim, K. H., Quah, C. C., Kim, W. R., and Shahimi, M. (2017). Anti-inflammatory potential of ellagic acid, gallic acid and punicalagin A&B isolated from *Punica granatum*. *BMC Complement Altern. Med.* 17, 1–10. doi: 10.1186/s12906-017-1555-0
- Boykin, J. V. Jr (2010). Wound nitric oxide bioactivity: a promising diagnostic indicator for diabetic foot ulcer management. *J. Wound Ostomy Continence Nurs.* 37, 25–32. doi: 10.1097/WON.0b013e3181c68b61
- Brennan, M., Bhatti, H., Nerusu, K. C., Bhagavathula, N., Kang, S., Fisher, G. J., et al. (2003). Matrix metalloproteinase-1 is the major collagenolytic enzyme responsible for collagen damage in UV-irradiated human skin. *Photochem. Photobiol.* 78, 43–48. doi: 10.1562/0031-8655(2003)078<0043:MMITMC>2.0.CO;2
- Brown, G. D., Denning, D. W., Gow, N. A., Levitz, S. M., Netea, M. G., and White, T. C. (2012). Hidden killers: human fungal infections. *Sci. Transl. Med.* 4, 165rv113–165rv113. doi: 10.1126/science.1222326
- Brown, P. K., Qureshi, A. T., Moll, A. N., Hayes, D. J., and Monroe, W. T. (2013). Single-cell analysis using hyperspectral imaging modalities. *ACS nano.* 7, 2948. doi: 10.1021/nn304868y
- Bruna, T., Maldonado-Bravo, F., Jara, P., and Caro, N. (2021). Silver nanoparticles and their antibacterial applications. *Int. J. Mol. Sci.* 22, 7202. doi: 10.3390/ijms22137202
- Bryan, N., Ahswin, H., Smart, N., Bayon, Y., Wohlert, S., and Hunt, J. A. (2012). Reactive oxygen species (ROS)—a family of fate deciding molecules pivotal in constructive inflammation and wound healing. *Eur. Cell Mater* 24, e65. doi: 10.22203/eCM.v024a18
- Canaparo, R., Foglietta, F., Limongi, T., and Serpe, L. (2020). Biomedical applications of reactive oxygen species generation by metal nanoparticles. *Materials* 14, 53. doi: 10.3390/ma14010053
- Carneiro, C. C., da Costa Santos, S., de Souza Lino, R. Jr, Bara, M. T. F., Chaibub, B. A., de Melo Reis, P. R., et al. (2016). Chemopreventive effect and angiogenic activity of punicalagin isolated from leaves of *Lafoesia pacari* A. St.-Hil. *Toxicol. Appl. Pharmacol.* 310, 1–8. doi: 10.1016/j.taap.2016.08.015
- Cheng, G., Wozniak, K., Wallig, M. A., Fidel, P. L. Jr., Trupin, S. R., and Hoyer, L. L. (2005). Comparison between *Candida albicans* agglutinin-like sequence gene expression patterns in human clinical specimens and models of vaginal candidiasis. *Infect. Immun.* 73, 1656–1663. doi: 10.1128/IAI.73.3.1656-1663.2005
- Chithra, P., Sajithlal, G., and Chandrakasan, G. (1998). Influence of Aloe vera on collagen characteristics in healing dermal wounds in rats. *Mol. Cell Biochem.* 181, 71–76. doi: 10.1023/A:1006813510959
- Choi, D. S., Kim, S., Lim, Y.-M., Gwon, H.-J., Park, J. S., Nho, Y.-C., et al. (2012). Hydrogel incorporated with chestnut honey accelerates wound healing and promotes early HO-1 protein expression in diabetic (db/db) mice. *Tissue Eng. Regenerative Med.* 9, 36–42. doi: 10.1007/s13770-012-0036-2
- Clinical and Laboratory Standards Institute (2012). *Methods for Dilution Antimicrobial Susceptibility Tests for Bacteria That Grow Aerobically; Approved Standard—Ninth Edition*. CLSI document M07-A9. Pennsylvania, United States: Clinical and Laboratory Standards Institute.
- Colombo, E., Sangiovanni, E., and Dell' Agli, M. (2013). A review on the anti-inflammatory activity of pomegranate in the gastrointestinal tract. *Evidence-Based Complementary Altern. Med.* 2013, 247145. doi: 10.1155/2013/247145
- Crivellato, E. (2011). The role of angiogenic growth factors in organogenesis. *Int. J. Dev. Biol.* 55, 365–375. doi: 10.1387/ijdb.103214ec
- Dahham, S. S., Ali, M. N., Tabassum, H., and Khan, M. (2010). Studies on antibacterial and antifungal activity of pomegranate (*Punica granatum* L.). *Am. Eurasian J. Agric. Environ. Sci.* 9, 273–281.
- Dai, J., Shen, J., Chai, Y., and Chen, H. (2021). IL-1 β impaired diabetic wound healing by regulating MMP-2 and MMP-9 through the p38 pathway. *Mediators Inflammation* 2021, 1–10. doi: 10.1155/2021/6645766
- Das, A., Kumar, A., Patil, N. B., Viswanathan, C., and Ghosh, D. (2015). Preparation and characterization of silver nanoparticle loaded amorphous hydrogel of carboxymethylcellulose for infected wounds. *Carbohydr Polym.* 130, 254–261. doi: 10.1016/j.carbpol.2015.03.082
- de Almeida Rochelle, S. L., Sardi, J., Freires, I. A., de Carvalho Galvão, L. C., Lazarini, J. G., de Alencar, S. M., et al. (2016). The anti-biofilm potential of commonly discarded agro-industrial residues against opportunistic pathogens. *Ind. Crops Products* 87, 150–160. doi: 10.1016/j.indcrop.2016.03.044
- de Oliveira, J. R., de Castro, V. C., Vilela, P. D. G. F., Camargo, S. E. A., Carvalho, C. A. T., Jorge, A. O. C., et al. (2013). Cytotoxicity of Brazilian plant extracts against oral microorganisms of interest to dentistry. *BMC Complement Altern. Med.* 13, 1–7.
- Dulińska-Litewka, J., Dykas, K., Felkle, D., Karnas, K., Khachatryan, G., and Karewicz, A. (2021). Hyaluronic acid-silver nanocomposites and their biomedical applications: A review. *Materials* 15, 234. doi: 10.3390/ma150102342
- Dunnill, C., Patton, T., Brennan, J., Barrett, J., Dryden, M., Cooke, J., et al. (2017). Reactive oxygen species (ROS) and wound healing: the functional role of ROS and emerging ROS-modulating technologies for augmentation of the healing process. *Int. Wound J.* 14, 89–96. doi: 10.1111/iwj.2017.14.issue-1
- Dwivedi, D., Dwivedi, M., Malviya, S., and Singh, V. (2017). Evaluation of wound healing, anti-microbial and antioxidant potential of *Pongamia pinnata* in wistar rats. *J. traditional complementary Med.* 7, 79–85. doi: 10.1016/j.jtcm.2015.12.002
- Dwivedi, S., Wahab, R., Khan, F., Mishra, Y. K., Musarrat, J., and Al-Khedhairi, A. A. (2014). Reactive oxygen species mediated bacterial biofilm inhibition via zinc oxide nanoparticles and their statistical determination. *PLoS One* 9, e111289. doi: 10.1371/journal.pone.0111289
- El-Aassar, M., Ibrahim, O. M., Fouda, M. M., El-Beheri, N. G., and Agwa, M. M. (2020). Wound healing of nanofiber comprising Polygalacturonic/Hyaluronic acid embedded silver nanoparticles: *In-vitro* and *in-vivo* studies. *Carbohydr Polym.* 238, 116175. doi: 10.1016/j.carbpol.2020.116175
- Elbially, Z. I., Atiba, A., Abdelnaby, A., Al-Hawary, I. I., Elsheshtawy, A., El-Serehy, H. A., et al. (2020). Collagen extract obtained from Nile tilapia (*Oreochromis niloticus* L.) skin accelerates wound healing in rat model via up regulating VEGF, bFGF, and α -SMA genes expression. *BMC Vet. Res.* 16, 1–11. doi: 10.1186/s12917-020-02566-2
- El Gazerly, H., Elbardisey, D. M., Eltokhy, H. M., and Teama, D. (2013). Effect of transforming growth factor Beta 1 on wound healing in induced diabetic rats. *Int. J. Health Sci.* 7, 160. doi: 10.12816/0006040
- El-Missiry, M. A., Amer, M. A., Hemieda, F. A., Othman, A. I., Sakr, D. A., and Abdulhadi, H. L. (2015). Cardioameliorative effect of punicalagin against streptozotocin-induced apoptosis, redox imbalance, metabolic changes and inflammation. *Egyptian J. Basic Appl. Sci.* 2, 247–260. doi: 10.1016/j.ejbas.2015.09.004
- Elzayat, E. M., Auda, S. H., Alanazi, F. K., and Al-Agamy, M. H. (2018). Evaluation of wound healing activity of henna, pomegranate and myrrh herbal ointment blend. *Saudi Pharm. J.* 26, 733–738. doi: 10.1016/j.sps.2018.02.016
- Firooz, A., Nafisi, S., and Maibach, H. I. (2015). Novel drug delivery strategies for improving econazole antifungal action. *Int. J. Pharm.* 495, 599–607. doi: 10.1016/j.ijpharm.2015.09.015
- Gallagher, K. A., Liu, Z.-J., Xiao, M., Chen, H., Goldstein, L. J., Buerk, D. G., et al. (2007). Diabetic impairments in NO-mediated endothelial progenitor cell mobilization and homing are reversed by hyperoxia and SDF-1 α . *J. Clin. Invest.* 117, 1249–1259. doi: 10.1172/JCI29710
- Gil, J., Solis, M., Higa, A., and Davis, S. C. (2022). *Candida albicans* Infections: a novel porcine wound model to evaluate treatment efficacy. *BMC Microbiol.* 22, 1–9. doi: 10.1186/s12866-022-02460-x
- Gorup, L. F., Longo, E., Leite, E. R., and Camargo, E. R. (2011). Moderating effect of ammonia on particle growth and stability of quasi-monodisperse silver nanoparticles synthesized by the Turkevich method. *J. Colloid Interface Sci.* 360 (2), 355–358. doi: 10.1016/j.jcis.2011.04.099
- Hu, Y., Xiong, Y., Zhu, Y., Zhou, F., Liu, X., Chen, S., et al. (2023). Copper-epigallocatechin gallate enhances therapeutic effects of 3D-printed dermal scaffolds in mitigating diabetic wound scarring. *ACS Appl. Materials Interfaces* 15, 38230–38246. doi: 10.1021/acsami.3c04733
- Ismail, T., Sestili, P., and Akhtar, S. (2012). Pomegranate peel and fruit extracts: a review of potential anti-inflammatory and anti-infective effects. *J. Ethnopharmacol.* 143, 397–405. doi: 10.1016/j.jep.2012.07.004
- Ivashchenko, O., Przywiecka, I., Peplińska, B., Jarek, M., Coy, E., and Jurga, S. (2018). Gel with silver and ultrasmall iron oxide nanoparticles produced with *Amanita muscaria* extract: physicochemical characterization, microstructure analysis and anticancer properties. *Sci. Rep.* 8, 13260. doi: 10.1038/s41598-018-31686-x
- Jindam, A., Yerra, V. G., and Kumar, A. (2017). Nrf2: a promising trove for diabetic wound healing. *Ann. Trans. Med.* 5, 469. doi: 10.21037/atm.2017.09.03
- Joshi, A. S., Singh, P., and Mijakovic, I. (2020). Interactions of gold and silver nanoparticles with bacterial biofilms: Molecular interactions behind inhibition and resistance. *Int. J. Mol. Sci.* 21, 7658. doi: 10.3390/ijms21207658
- Karim, S., Alkreathy, H. M., Ahmad, A., and Khan, M. I. (2021). Effects of methanolic extract based-gel from Saudi pomegranate peels with enhanced healing potential on excision wounds in diabetic rats. *Front. Pharmacol.* 12, 704503. doi: 10.3389/fphar.2021.704503
- Kataoka, M., Minami, K., Takagi, T., Amidon, G. E., and Yamashita, S. (2021). *In vitro-in vivo* correlation in cocrystal dissolution: consideration of drug release profiles based on coformer dissolution and absorption behavior. *Mol. Pharm.* 18, 4122–4130. doi: 10.1021/acs.molpharmaceut.1c00537
- Kaur, R., Mehan, S., Khanna, D., and Kalra, S. (2015). Polyphenol ellagic acid—targeting to brain: A hidden treasure. *Int. J. Neurol. Res.* 1, 141–152.
- Kiritisi, D., and Nyström, A. (2018). The role of TGF β in wound healing pathologies. *Mech. Ageing Dev.* 172, 51–58. doi: 10.1016/j.mad.2017.11.004
- Kurtzman, C. P., Fell, J. W., Boekhout, T., and Robert, V. (2011). “Methods for isolation, phenotypic characterization and maintenance of yeasts,” in *The yeasts* (Amsterdam: Elsevier), 87–110.
- Kushwaha, A., Goswami, L., and Kim, B. S. (2022). Nanomaterial-based therapy for wound healing. *Nanomaterials* 12, 618. doi: 10.3390/nano12040618
- Lara, H., Romero-Urbina, D. G., Pierce, C., Lopez-Ribot, J. L., and Josefina, M. (2015). Arellano-Jiménez and M Jose-Yacaman Effect of silver nanoparticles on *Candida albicans* biofilms: an ultrastructural study. *J. Nanobiotechnol.* 13, 91. doi: 10.1186/s12951-015-0147-8
- Lázaro-Martínez, J. L., Álvaro-Afonso, F. J., Sevillano-Fernández, D., Molines-Barroso, R. J., García-Álvarez, Y., and García-Morales, E. (2019). Clinical and antimicrobial efficacy of a silver foam dressing with silicone adhesive in diabetic foot ulcers with mild infection. *Int. J. Lower Extremity Wounds* 18, 269–278. doi: 10.1177/1534734619866610
- Lee, E. J., Lee, J. H., Jin, L., Jin, O. S., Shin, Y. C., Oh, S. J., et al. (2014). Hyaluronic acid/poly (lactic-co-glycolic acid) core/shell fiber meshes loaded with epigallocatechin-

- 3-O-gallate as skin tissue engineering scaffolds. *J. Nanoscience Nanotechnology* 14, 8458–8463. doi: 10.1166/jnn.2014.9922
- Liu, T., Han, M., Tian, F., Cun, D., Rantanen, J., and Yang, M. (2018). Budesonide nanocrystal-loaded hyaluronic acid microparticles for inhalation: *in vitro* and *in vivo* evaluation. *Carbohydr Polym* 181, 1143–1152. doi: 10.1016/j.carbpol.2017.11.018
- Liu, X., Lee, Py, Ho, Cm, Lui, V. C., Chen, Y., Che, Cm, et al. (2010). Silver nanoparticles mediate differential responses in keratinocytes and fibroblasts during skin wound healing. *ChemMedChem* 5, 468–475. doi: 10.1002/cmdc.200900502
- Livak, K. J., and Schmittgen, T. D. (2001). Analysis of relative gene expression data using real-time quantitative PCR and the $2^{-\Delta\Delta CT}$ method. *Methods* 25, 402–408. doi: 10.1006/meth.2001.1262
- Loboda, A., Damulewicz, M., Pyza, E., Jozkowicz, A., and Dulak, J. (2016). Role of Nrf2/HO-1 system in development, oxidative stress response and diseases: an evolutionarily conserved mechanism. *Cell Mol. Life Sci.* 73, 3221–3247. doi: 10.1007/s00108-016-2223-0
- Long, M., Rojo de la Vega, M., Wen, Q., Bharara, M., Jiang, T., Zhang, R., et al. (2016). An essential role of NRF2 in diabetic wound healing. *Diabetes* 65, 780–793. doi: 10.2337/db15-0564
- Loreto, F., and Velikova, V. (2001). Isoprene produced by leaves protects the photosynthetic apparatus against ozone damage, quenches ozone products, and reduces lipid peroxidation of cellular membranes. *Plant Physiol.* 127, 1781–1787. doi: 10.1104/pp.010497
- Luengo, J., Weiss, B., Schneider, M., Ehlers, A., Stracke, F., König, K., et al. (2006). Influence of nanoencapsulation on human skin transport of flufenamic acid. *Skin Pharmacol. Physiol.* 19, 190–197. doi: 10.1159/000093114
- Lukiswanto, B. S., Miranti, A., Sudjarwo, S. A., Primarizky, H., and Yuniarti, W. M. (2019). Evaluation of wound healing potential of pomegranate (*Punica granatum*) whole fruit extract on skin burn wound in rats (*Rattus norvegicus*). *J. advanced veterinary Anim. Res.* 6, 202. doi: 10.5455/javar.2019.f333
- Makvand, P., Ali, G. W., Della Sala, F., Abdel-Fattah, W. I., and Borzacchiello, A. (2019). Biosynthesis and characterization of antibacterial thermosensitive hydrogels based on corn silk extract, hyaluronic acid and nanosilver for potential wound healing. *Carbohydr Polym* 223, 115023. doi: 10.1016/j.carbpol.2019.115023
- Masoko, P., Picard, J., Howard, R., Mampuru, L., and Eloff, J. (2010). *In vivo* antifungal effect of Combretum and Terminalia species extracts on cutaneous wound healing in immunosuppressed rats. *Pharm. Biol.* 48, 621–632. doi: 10.3109/13880200903229080
- Minghetti, P., Cilurzo, F., Casiraghi, A., and Montanari, L. (2006). Evaluation of *ex vivo* human skin permeation of gelsein and daidzein. *Drug Delivery* 13, 411–415. doi: 10.1080/10717540500466089
- Nailis, H., Kuchariková, S., Řičicová, M., Van Dijk, P., Deforce, D., Nelis, H., et al. (2010). Real-time PCR expression profiling of genes encoding potential virulence factors in *Candida albicans* biofilms: identification of model-dependent and -independent gene expression. *BMC Microbiol.* 10, 1–11. doi: 10.1186/1471-2180-10-114
- Nayak, S. B., Isik, K., and Marshall, J. R. (2017). Wound-Healing potential of oil of *Hypericum perforatum* in excision wounds of male sprague dawley rats. *Adv. Wound Care* 6, 401–406. doi: 10.1089/wound.2017.0746
- Nirwana, I., Munadziroh, E., Yuliati, A., Fadhila, A. I., Wardhana, A. S., Shariff, K. A., et al. (2022). Ellagic acid and hydroxyapatite promote angiogenesis marker in bone defect. *J. Oral. Biol. Craniofacial Res.* 12, 116–120. doi: 10.1016/j.jobcr.2021.11.008
- Okur, M. E., Karantas, I. D., Şenyigit, Z., Okur, N.Ü., and Sifağa, P. I. (2020). Recent trends on wound management: New therapeutic choices based on polymeric carriers. *Asian J. Pharm. Sci.* 15, 661–684. doi: 10.1016/j.ajps.2019.11.008
- Olczyk, P., Mencner, Ł., and Komosińska-Vassev, K. (2014). The role of the extracellular matrix components in cutaneous wound healing. *BioMed. Res. Int* 2014, 747584. doi: 10.1155/2014/747584
- Ortega, S., Ittmann, M., Tsang, S. H., Ehrlich, M., and Basilio, C. (1998). Neuronal defects and delayed wound healing in mice lacking fibroblast growth factor 2. *Proc. Natl. Acad. Sci.* 95, 5672–5677. doi: 10.1073/pnas.95.10.5672
- Özkan, M., Kirca, A., and Cemeroglu, B. (2004). Effects of hydrogen peroxide on the stability of ascorbic acid during storage in various fruit juices. *Food Chem.* 88, 591–597. doi: 10.1016/j.foodchem.2004.02.011
- Paczowska-Walendowska, M., Ignacyk, M., Miklaszewski, A., Plech, T., Karpiński, T. M., Kwiatek, J., et al. (2024). Electrospun nanofibers with pomegranate peel extract as a new concept for treating oral infections. *Materials* 17, 2558. doi: 10.3390/ma17112558
- Patra, J. K., and Baek, K.-H. (2017). Antibacterial activity and synergistic antibacterial potential of biosynthesized silver nanoparticles against foodborne pathogenic bacteria along with its anticandidal and antioxidant effects. *Front. Microbiol.* 8, 227226. doi: 10.3389/fmicb.2017.00167
- Perween, N., Khan, H., and Fatima, N. (2019). Silver nanoparticles: an upcoming therapeutic agent for the resistant *Candida* infections. *J. Microbiol. Exp.* 7, 49–54. doi: 10.15406/jmen.2019.07.00240
- Raina, N., Rani, R., Thakur, V. K., and Gupta, M. (2023). New insights in topical drug delivery for skin disorders: from a nanotechnological perspective. *ACS omega* 8, 19145–19167. doi: 10.1021/acsomega.2c08016
- Ruffo, M., Parisi, O. I., Dattilo, M., Patitucci, F., Malivindi, R., Pezzi, V., et al. (2022). Synthesis and evaluation of wound healing properties of hydro-diab hydrogel loaded with green-synthesized AGNPs: *in vitro* and *in vivo* studies. *Drug Delivery Transl. Res.* 12 (8), 1881–1894. doi: 10.1007/s13346-022-01121-w
- Sadeghian, A., Ghorbani, A., Mohamadi-Nejad, A., and Rakhshandeh, H. (2011). Antimicrobial activity of aqueous and methanolic extracts of pomegranate fruit skin. *Avicenna J. Phytomedicine* 1, 67–73. doi: 10.22038/AJP.2011.123
- Salama, A. A., Ismael, N. M., and Bedewy, M. (2021). The anti-inflammatory and antiatherogenic *in vivo* effects of pomegranate peel powder: from waste to medicinal food. *J. Med. Food* 24, 145–150. doi: 10.1089/jmf.2019.0269
- Santos, S. C. R., Miguel, C., Domingues, I., Calado, A., Zhu, Z., Wu, Y., et al. (2007). VEGF and VEGFR-2 (KDR) internalization is required for endothelial recovery during wound healing. *Exp. Cell Res.* 313, 1561–1574. doi: 10.1016/j.yexcr.2007.02.020
- Sayed, S., Alotaibi, S. S., El-Shehawi, A. M., Hassan, M. M., Shukry, M., Alkafafy, M., et al. (2022). The anti-inflammatory, anti-apoptotic, and antioxidant effects of a pomegranate-peel extract against acrylamide-induced hepatotoxicity in rats. *Life* 12, 224. doi: 10.3390/life12020224
- Scappaticci, R. A. F., Berretta, A. A., Torres, E. C., Buszinski, A. F. M., Fernandes, G. L., Dos Reis, T. F., et al. (2021). Green and chemical silver nanoparticles and pomegranate formulations to heal infected wounds in diabetic rats. *Antibiotics* 10, 1343. doi: 10.3390/antibiotics10111343
- Scheller, J., Chalaris, A., Schmidt-Arras, D., and Rose-John, S. (2011). The pro-and anti-inflammatory properties of the cytokine interleukin-6. *Biochim. Biophys. Acta (BBA)-Molecular Cell Res.* 1813, 878–888. doi: 10.1016/j.bbamer.2011.01.034
- Seeram, N. P., Zhang, Y., Reed, J. D., Krueger, C. G., and Vaya, J. (2006). “Pomegranate phytochemicals,” in *Pomegranates* (Cambridge: CRC Press), 21–48.
- Shafique, M., Khan, M. A., Khan, W. S., Ahmad, W., and Khan, S. (2017). Fabrication, characterization, and *in vivo* evaluation of famotidine loaded solid lipid nanoparticles for boosting oral bioavailability. *J. Nanomaterials* 2017, 7357150. doi: 10.1155/2017/7357150
- Shalumon, K., Sheu, C., Chen, C.-H., Chen, S.-H., Jose, G., Kuo, C.-Y., et al. (2018). Multi-functional electrospun antibacterial core-shell nanofibrous membranes for prolonged prevention of post-surgical tendon adhesion and inflammation. *Acta Biomater* 72, 121–136. doi: 10.1016/j.actbio.2018.03.044
- Shen, H.-M., Chen, C., Jiang, J.-Y., Zheng, Y.-L., Cai, W.-F., Wang, B., et al. (2017). The N-butyl alcohol extract from *Hibiscus rosa-sinensis* L. flowers enhances healing potential on rat excisional wounds. *J. Ethnopharmacol* 198, 291–301. doi: 10.1016/j.jep.2017.01.016
- Simonsen, L., Petersen, M. B., and Groth, L. (2002). *In vivo* skin penetration of salicylic compounds in hairless rats. *Eur. J. Pharm. Sci.* 17, 95–104. doi: 10.1016/S0928-0987(02)00147-1
- Skłodowski, K., Chmielewska-Deptuła, S. J., Piktel, E., Wolak, P., Wollny, T., and Bucki, R. (2023). Metallic nanosystems in the development of antimicrobial strategies with high antimicrobial activity and high biocompatibility. *Int. J. Mol. Sci.* 24, 2104. doi: 10.3390/ijms24032104
- Sreekumar, S., Sithul, H., Muralidharan, P., Azeez, J. M., and Sreeharshan, S. (2014). Pomegranate fruit as a rich source of biologically active compounds. *BioMed. Res. Int.* 2014, 686921. doi: 10.1155/2014/686921
- Taff, H. T., Mitchell, K. F., Edward, J. A., and Andes, D. R. (2013). Mechanisms of *Candida* biofilm drug resistance. *Future Microbiol.* 8, 1325–1337. doi: 10.2217/fmb.13.101
- Tarusha, L., Paoletti, S., Travan, A., and Marsich, E. (2018). Alginate membranes loaded with hyaluronic acid and silver nanoparticles to foster tissue healing and to control bacterial contamination of non-healing wounds. *J. Mater. Sci. Mater. Med.* 29, 1–14. doi: 10.1007/s10856-018-6027-7
- Tayel, A. A., and El-Tras, W. F. (2010). Anticandidal activity of pomegranate peel extract aerosol as an applicable sanitizing method. *Mycoses* 53, 117–122. doi: 10.1111/j.1439-0507.2008.01681.x
- Tsang, P. W.-K., Bandara, H., and Fong, W.-P. (2012). Purpurin suppresses *Candida albicans* biofilm formation and hyphal development. *PLoS One* 7, e50866. doi: 10.1371/journal.pone.0050866
- Um, I. C., Fang, D., Hsiao, B. S., Okamoto, A., and Chu, B. (2004). Electro-spinning and electro-blending of hyaluronic acid. *Biomacromolecules* 5, 1428–1436. doi: 10.1021/bm034539b
- Urciuolo, F., Casale, C., Imparato, G., and Netti, P. A. (2019). Bioengineered skin substitutes: the role of extracellular matrix and vascularization in the healing of deep wounds. *J. Clin. Med.* 8, 2083. doi: 10.3390/jcm8122083
- Vazquez-Muñoz, R., Avalos-Borja, M., and Castro-Longoria, E. (2014). Ultrastructural analysis of *Candida albicans* when exposed to silver nanoparticles. *PLoS One* 9, e108876. doi: 10.1371/journal.pone.0108876
- Venusova, E., Kolesarova, A., Horky, P., and Slama, P. (2021). Physiological and immune functions of punicalagin. *Nutrients* 13, 2150. doi: 10.3390/nu13072150
- Wang, P. H., Huang, B.-S., Horng, H.-C., Yeh, C.-C., and Chen, Y.-J. (2018). Wound healing. *J. Chin. Med. Assoc.* 2, 94–101. doi: 10.1016/j.jcma.2017.11.002
- Wang, Z., Ou, X., Guan, L., Li, X., Liu, A., Li, L., et al. (2023). Pomegranate-inspired multifunctional nanocomposite wound dressing for intelligent self-monitoring and promoting diabetic wound healing. *Biosens. Bioelectron.* 235, 115386. doi: 10.1016/j.bios.2023.115386
- Witte, M. B., and Barbul, A. (2002). Role of nitric oxide in wound repair. *Am. J. Surg.* 183, 406–412. doi: 10.1016/s0002-9610(02)00815-2
- Yeligar, S. M., Machida, K., and Kalra, V. K. (2010). Ethanol-induced HO-1 and NQO1 are differentially regulated by HIF-1 α and Nrf2 to attenuate inflammatory cytokine expression. *J. Biol. Chem.* 285, 35359–35373.
- Yuniarti, W. M., Primarizky, H., and Lukiswanto, B. S. (2018). The activity of pomegranate extract standardized 40% ellagic acid during the healing process of incision wounds in albino rats (*Rattus norvegicus*). *Veterinary world.* 11, 321.

Zhang, Y., Liu, Y.-C., Chen, S.-M., Jiang, Y.-Y., and An, M.-M. (2021). Evaluation of the *in vitro* activity and *in vivo* efficacy of anidulafungin-loaded human serum albumin nanoparticles against *Candida albicans*. *Front. Microbiol.* 12, 788442. doi: 10.3389/fmicb.2021.788442

Zhao, Q., Xu, J., and Cheng, Z. (2023). Growth differentiation factor 10 induces angiogenesis to promote wound healing in rats with diabetic foot ulcers by activating

TGF- β 1/Smad3 signaling pathway. *Front. Endocrinol. (Lausanne)* 13, 1013018. doi: 10.3389/fendo.2022.1013018

Zhou, J., Ni, M., Liu, X., Ren, Z., and Zheng, Z. (2017). Curcumin promotes vascular endothelial growth factor (VEGF)-mediated diabetic wound healing in streptozotocin-induced hyperglycemic rats. *Med. Sci. Monitor: Int. Med. J. Exp. Clin. Res.* 23, 555. doi: 10.12659/MSM.902859